

Additive Nanomanufacturing – A Review

D. S. Engstrom, B. Porter, M. Pacios and H. Bhaskaran*

Department of Materials, University of Oxford, 16 Parks Road, OX1 3PH, Oxford, UK

Abstract

Additive manufacturing has provided a pathway for inexpensive and flexible manufacturing of specialized components and one-off parts. At the nanoscale, such techniques are less ubiquitous. Manufacturing at the nanoscale is dominated by lithography tools that are too expensive for small and medium size enterprises (SMEs) to invest in. Additive nanomanufacturing (ANM) empowers smaller facilities to design, create and manufacture on their own while providing a wider material selection and flexible design. This is especially important as nanomanufacturing thus far is largely constrained to 2-dimensional patterning techniques and being able to manufacture in 3-dimensions could open up new concepts. In this review we outline the state-of-the-art within ANM technologies such as Electrohydrodynamic Jet Printing, Dip-pen Lithography, Direct Laser Writing, and several single particle placement methods such as Optical Tweezers and Electrokinetic nanomanipulation. The ANM technologies are compared in terms of deposition speed, resolution and material selection and finally a prospectus of ANM in the future is given. This review is up-to-date until April 2014.

1. Introduction

Nanoscale manufacturing techniques are essential to live up to the promises made on the prospects of nanotechnology; without methods to rapidly fabricate and test new concepts, innovation in this emerging field can be stifled. Additive manufacturing is already employed at the macro scale for rapid prototyping and low volume production in areas such as dental and medical care, automotive, aerospace, fashion, and entertainment.¹ These areas have benefited from the freedom of design and reduced time-to-market provided by additive manufacturing. Unfortunately, such rapid prototyping techniques are yet to be developed for nanomanufacturing. Such a technology would have the potential to transform manufacturing on the nanoscale as well. Within the scientific community the focus has been on tissue engineering,^{2, 3} electronics,^{4, 5}

*Corresponding author: harish.bhaskaran@materials.ox.ac.uk

microfluidics,^{6, 7} orthopaedics,^{8, 9} health care,^{10, 11} and materials,¹² but as the resolution improves more applications such as photovoltaics,^{13, 14} optics,¹⁵ and nanoelectronics^{16, 17} are emerging.

For decades, realistic options for full scale industrial nanomanufacturing have relied on photolithography using electromagnetic radiation with increasingly shorter wavelength.¹⁸ The equipment to reach nanometre dimensions reliably is, however, prohibitively expensive, thereby excluding smaller R&D facilities and small and medium enterprises (SMEs) from taking advantage of their innovations. Electron beam lithography (EBL) offers flexibility and high resolution¹⁹ for R&D and is comparably cheap but is still only affordable for well-funded universities and companies with large capital investments. Device fabrication using both photolithography and EBL relies on exposures of multiple layers of polymer thin films. These are planar technologies operating virtually only in two dimensions; developing fabrication methods that extend into the third dimension seems an obvious way to save space, cost and to gain additional functionality. Moreover, the lift-off and etching processes related to resist based manufacturing are extremely wasteful as only a small percentage of the used materials is turned into functional elements.²⁰ Additive nanomanufacturing (ANM) does not seek to replace the resist-based planar manufacturing methods used for integrated circuit (IC) fabrication, but rather seeks to add functionally in ways these technologies cannot. More importantly, it could change the way we think about manufacturing at the nanoscale, which could also lead to much greater flexibility in the design.

Before we begin a technical review, we will define ANM as we perceive it for the purposes of this review. We define ANM as incorporating techniques that directly add the desired material in its final shape, with sub-100 nm resolution, without subtractive removal. This definition excludes thin film fabrication methods such as atomic layer deposition (ALD) and molecular beam epitaxy (MBE) although these methods might successfully be combined with additive manufacturing methods. ~~Direct laser writing, near-field optical lithography and plasmonic lensing are borderline ANM technologies, as these can produce structures in their final shape after an additional development process. For completeness these are included in the review. One exception has been made for direct laser writing, which is included despite being a lithography method, because it is the one technology that has so far created true three-dimensional nanostructures.~~

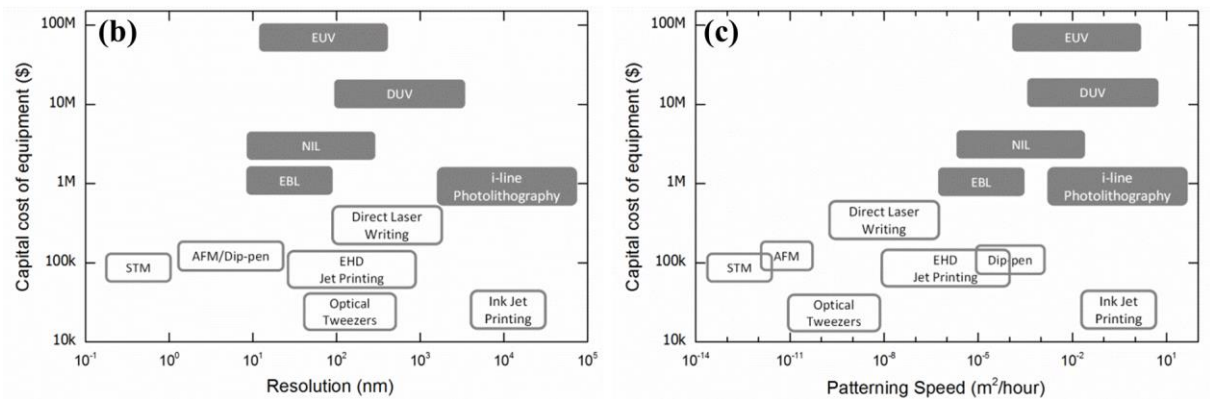
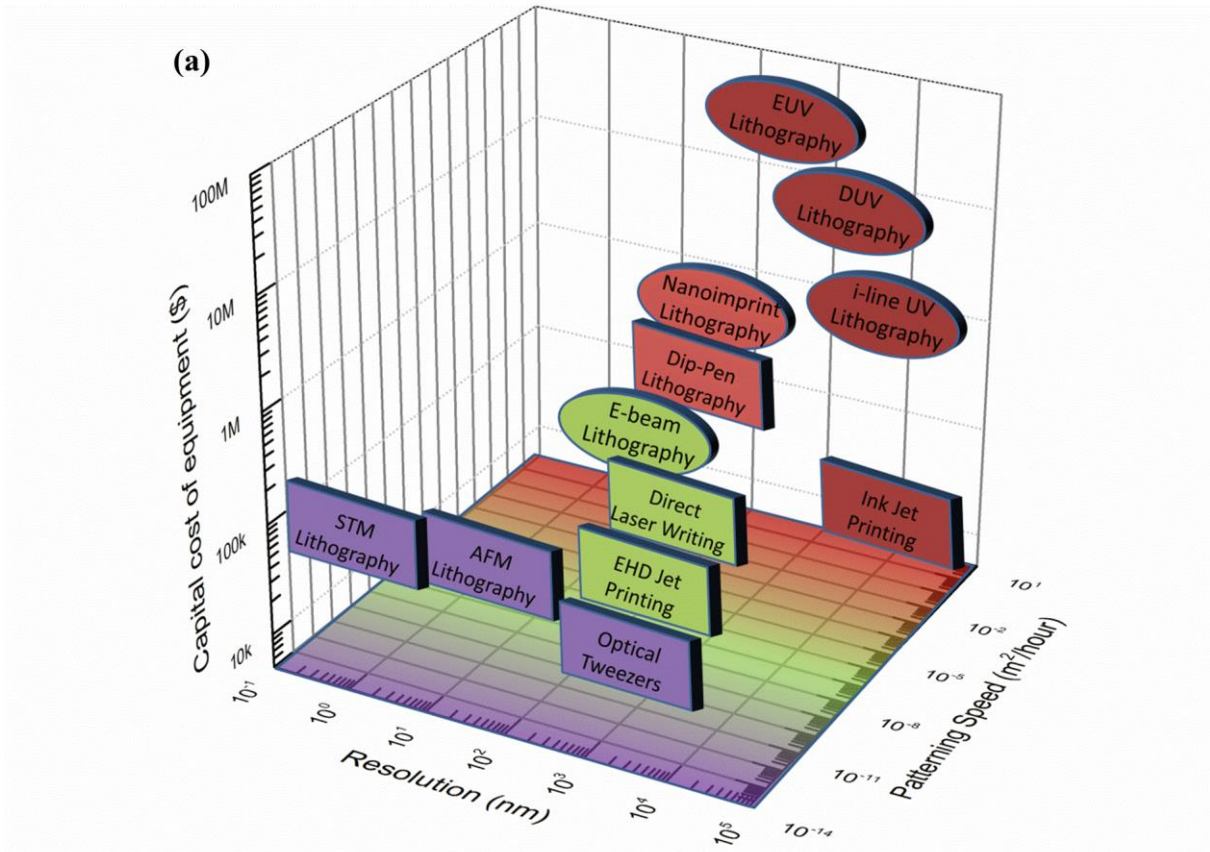


FIG. 1 (a) Equipment cost, patterning speed and minimum resolution of additive manufacturing methods (square) compared to traditional resist based lithography methods (ellipse). **(b)** Projection of the 3D graph in (a) showing the capital cost of equipment vs. minimum resolution for ANM methods (white) and traditional resist based methods (grey). **(c)** Projection of the 3D graph in (a) showing the capital cost of equipment vs. patterning speed for ANM methods (white) and traditional resist based methods (grey). (EUV = Extreme UV lithography, DUV = Deep UV Lithography, EBL = Electron-Beam Lithography, NIL = Nanoimprint Lithography, STM = Scanning Tunneling Microscopy, AFM = Atomic Force Microscopy).

The cost of thin film nanolithography tools is growing rapidly with equipment cost ranging from \$1 million to \$100 million for the latest extreme UV lithography tools. In FIG. 1 (a) the patterning speed, resolution and estimated capital equipment cost of ANM methods (square) are compared with traditional resist based thin film manufacturing methods (ellipse). The capital equipment cost for ANM methods are generally much

smaller than for resist based manufacturing methods without sacrificing resolution as clarified in FIG. 1 (b). This is one of the primary reasons ANM is envisioned to spread to SMEs and research labs. The price per unit can still be high for additive manufacturing¹ because of the relatively low patterning speed as shown in FIG. 1 (c); but for low volume and high value products, the comparatively low investment prospects of this technique can be particularly attractive.

When comparing manufacturing methods at the micro- and nanoscale, one often focuses on the resolution of the technology as it is closely linked to the performance of the product. For commercial use, resolution is, however, only one significant parameter as the ability to position structures relative to one another (accuracy/alignment), writing speed and materials are equally important.

Manufacturing at the nanoscale is very different from macroscale manufacturing because of fundamental physical limits. Therefore, the difficulties met are also very different. Fabrication at the nanoscale becomes a matter of manipulating very few atoms or molecules at a time and manufacturing variations of just a single atom or molecule can lead to catastrophic device failure. Additionally, structures with dimensions below 50 nm also have a reduced melting point which can affect their mechanical stability^{21, 22} and even defining alloy composition, doping levels and crystallinity becomes complex as the presence or spatial location of a single atom will change the material properties. At the nanoscale, gravity is insignificant and the dominating forces become the surface interactions such as van der Waals forces that can cause unwanted adhesion. In liquid, Brownian motion and convection forces are comparatively strong making particle capture difficult and even in air or vacuum vibrations from fans, pumps or passing traffic can render structural alignment impossible.

For ANM the challenge is to manufacture nanoscale structures at a large scale with great accuracy, high resolution, low cost and using materials ranging from biomaterials to ceramics and metals. However, ANM does not aim to compete with existing technologies and it can create new ways to manufacture and change the way we design products. In this review we focus on the range of ANM methods available today and the level they are at in terms of resolution, accuracy, speed and materials. We have divided the manufacturing methods into two groups: Direct Writing and Single Particle Placement. Within each group, the state-of-the-art ANM techniques will be described and evaluated and finally these techniques will be compared to provide an outlook on ANM and its prospects over the next decade.

2. Direct Writing

Direct writing of nanoscale devices composed of metals, insulators and organic materials is of interest for a range of ANM applications. Here we review recent advances in three key direct writing methods of nanostructures: dip-pen nanolithography (DPN), electrohydrodynamic direct writing (EHD), and direct laser writing (DLW). All three technologies are able to achieve sub-30 nm resolution, relatively high writing speed, and the capacity for 3-dimensional nanomanufacturing. The choice of materials, at least for DPN and EHD, is already vast ranging from metals to biomaterials and the material selection for direct laser writing is also increasing. In this section the promising future of direct writing ANM is outlined through examples of the state-of-the-art of each of these three technologies.

2.1 Dip-pen Nanolithography

Dip-pen Nanolithography (DPN) is a scanning probe microscopy-based flexible nanofabrication process for making 2-D nanoscale features that uniquely combines direct-write soft-matter compatibility with the high resolution and registry of atomic force microscopy (AFM), all in a mask-free and biocompatible system.²³ Originally, scanning probe microscopes (SPMs), such as the scanning tunnelling microscope (STM)²⁴ and the atomic force microscope (AFM),²⁵ emerged as nanoscale imaging and spectroscopic tools in the mid 1980s. Soon thereafter manipulation of single-atoms²⁶ and atom-by-atom construction of nanopatterns marked the birth of scanning probe lithography (SPL), suggesting that SPMs could indeed be used for molecular printing or perhaps even manufacturing.²⁷

Hereafter, a series of indirect SPL methods based on destructive delivery of energy to create functional patterns were developed. Taking advantage of the positioning resolution enabled by piezo-actuation and the nanoscale radii of the tips, scientists were able to generate sub-50-nm features by scratching, etching and oxidizing surfaces.²⁸ A process known as nanoshaving or nanografting uses the tip of an AFM and an applied force to remove a molecular monolayer on gold in a site-specific fashion²⁹ and anodic oxidation of silicon was developed by Quate and colleagues for patterning silicon substrates.^{30, 31}

In contrast to nanoshaving and nanografting DPN selectively transfers material from an ink coated probe tip on to a surface with a variety of ink-surface combinations.^{23, 32} A schematic of the process is shown in FIG. 2. Ink

molecules are transported via mass diffusion from the tip on to the surface. Features are formed on the surface via either chemisorption based self-assembly or physisorption.³³ Ink transport is mediated by the presence of the water meniscus that forms when the tip is brought in close proximity to the surface under ambient conditions. Due to the naturally occurring water meniscus for mass transfer this method also avoids the necessity for ultrahigh vacuum. Moreover, there is no need to expose the substrate to ultraviolet, ion- or electron-beam radiation, characteristic of indirect patterning techniques, and therefore DPN can be used to print fragile or reactive organic and biological materials.

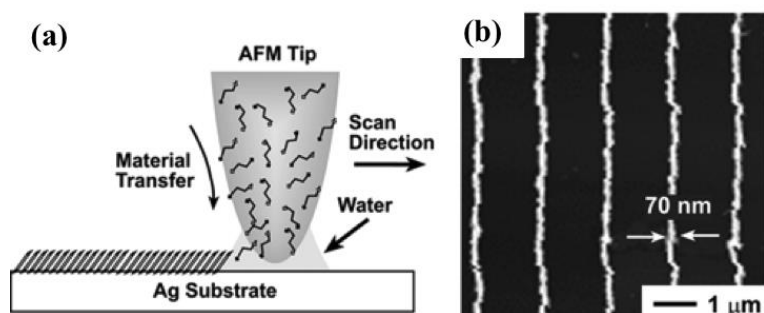


FIG. 2 (a) Schematic representation of the basic molecular deposition by DPN through a water meniscus formed between the scanning probe tip and the substrate surface. (b) Direct deposition of SAMs (16-mercaptohexadecanoic acid) on Ag as an etch resist to pattern 70-nm wide features. Reproduced from^{34, 35}.

From initial demonstrations involving alkanethiols on gold,³⁶ DPN has evolved into a versatile technique used to write or template both inorganic and organic nanostructures.^{23, 37} Polymers,³⁸ colloidal nanoparticles (e.g. magnetic nanocrystals and carbon nanotubes),^{39, 40, 41} electrodeposited metals,⁴² sol-gel precursors,⁴³ small organic molecules,^{44, 45} biomolecules (proteins^{46, 47} and oligonucleotides⁴⁸) and even single viruses⁴⁹ and bacteria have been patterned on a variety of substrates (including metals, semiconductors and insulators)³⁹ by controlling various experimental parameters such as ambient humidity, writing speed, and dwell time.^{50, 45} In fact, these experimental parameters serve a useful function of being the levers that control the features size. However, DPN initially faced a drawback common to other indirect SPLs of poor throughput. This was because the first incarnations of DPN were serial processes, and were thus lower in throughput than stamping or optical lithography-based techniques. In order to compete with these techniques, it was necessary to increase the throughput of DPN by parallelizing the deposition process. The scalability of DPN was demonstrated by Salaita et al.⁵¹ who were able to fabricate a 55,000-pen 2D array generating 88 million Au dots (pitch distance

400 nm) with a diameter equal to 100 ± 20 nm (See FIG. 3). This increased the throughput of DPN by four orders of magnitude, fabricating the 88 million dots in approximately 5 min. Even with impressive recent advances in cantilever array design, such arrays tend to be highly specialized for a given application. They are also mechanically fragile, expensive, and often difficult to implement. It is therefore difficult to imagine commercially viable production methods based on scanning probe systems that rely on conventional cantilevers.⁵² New scanning-probe contact-printing methods to reduce the cost barriers associated with massively parallel DPN were needed to achieve high-throughput and to define patterns with high-resolution.⁵³

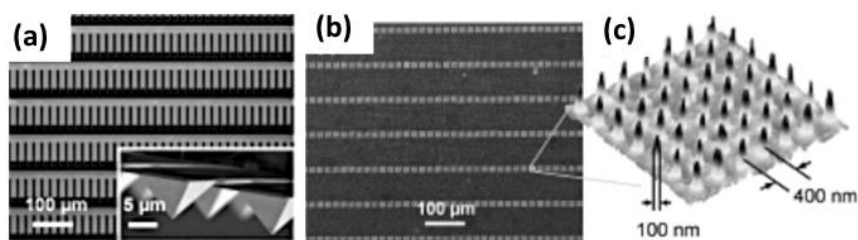


FIG. 3 (a) Optical micrograph of part of the 2D array of cantilevers used for patterning. Inset: SEM image of the cantilever arrays at a different viewing angle. (b) Large-area SEM image of part of an 88 000 000-gold-dot array (40×40 within each block) on an oxidized silicon substrate. (c) Representative AFM topographical image of part of one of the blocks, where the dot-to-dot distance is 400 nm, and the dot diameter is (100 ± 20) nm. Reproduced from⁵¹.

The second key advance in molecular printing was therefore to replace the cantilever with an elastomeric pyramid on a solid backing. This approach is called Polymer Pen Lithography (PPL) and is shown in FIG. 4.⁵⁴ The elastomeric tips can print a digitized pattern with spot sizes ranging from 90 nm to over 10 μm, simply by changing the force and time over which the ink is delivered. This feature-size dependence on force is a remarkably controllable parameter and distinguishes PPL from both DPN and conventional contact printing. Because the elastomeric tip array can absorb ink and act as a reservoir, it can be used to print over large areas and for multiple printing tasks without re-inking. The patterning capabilities have been demonstrated with arrays that contain anywhere between 15,000 to ~11,000,000 pyramid-shaped pens. PPL has also proven to be effective for patterning small molecules and proteins and has been used to make patterns of electronic circuits.⁵⁴

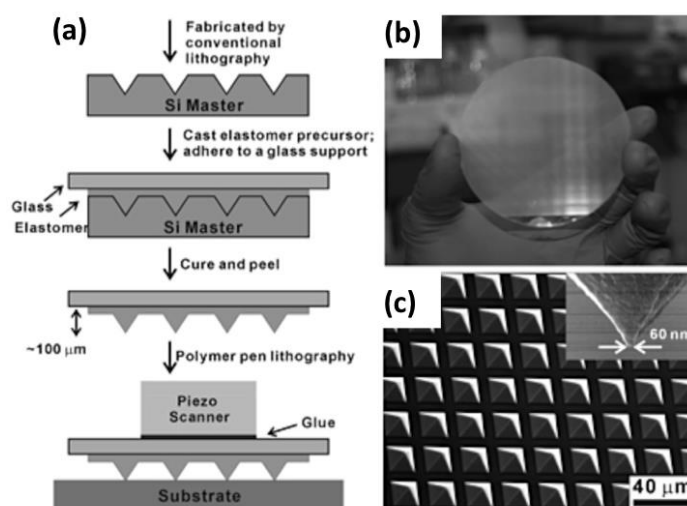


FIG. 4 (a) A schematic illustration of the polymer pen lithography setup. (b) A photograph of an 11-million-pen array. (c) Scanning electron microscope image of the polymer pen array. The average tip radius of curvature is 70 ± 10 nm (inset). Reproduced from⁵⁴.

A third key advance was to overcome the feature size limits of elastomeric pens in PPL by fabricating arrays of ultra-sharp Si tips on a spring-like elastomer layer that allows all of the tips to be brought into contact with a surface over large areas. This method is called Hard-tip, soft-spring lithography⁵² (HSL) and is illustrated in FIG. 5. In HSL there is a lack of feature diameter dependence on the force exerted between the tip array and the surface, because Si tips do not deform under pressure. However, there is a linear relationship between the feature area and the square root of the dwell time. HSL is also distinguished from all other lithographic techniques by the ability to form arbitrary patterns in massively parallel (over a 1-cm^2 area) and mask-less fashion at a feature resolution of less than 50 nm.

Other challenges such as the direct writing of single sub-10 nm nanoparticles in a specific location individually on a substrate have allowed further development of DPN. Scanning Probe Block Co-polymer Lithography (SPBCL)⁵⁵ relies on either DPN or PPL to transfer phase-separating block copolymer inks in the form of 100 nm or larger features on an underlying substrate. Reduction of the metal ions via plasma results in the high-yield formation of single crystal nanoparticles per block copolymer feature. For instance, integration of individual nanoparticles on devices⁵⁶ or single-molecule protein arrays⁵⁷ have been enabled by scanning probe block copolymer lithography.

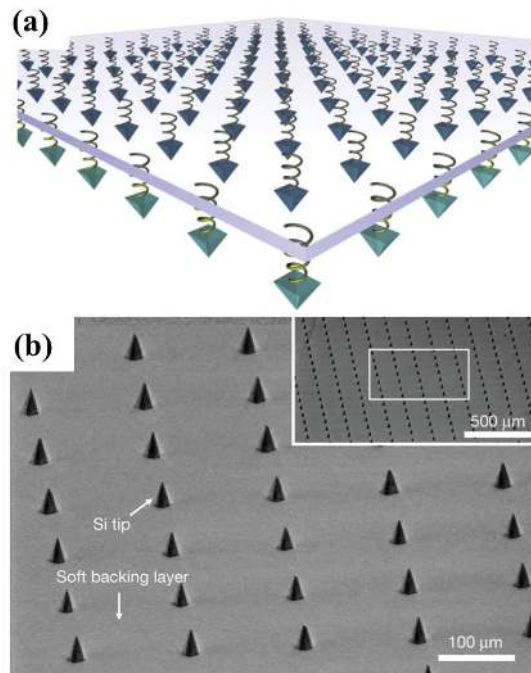


FIG. 5 (a) Schematic illustration of a Hard-tip, soft-spring lithography (HSL) tip array supported by a transparent, soft backing layer that provides mechanical flexibility to each tip. **(b)** An SEM image of the Si tip array on SiO₂/PDMS/glass with a 150- μ m pitch between tips. The inset shows a large area of the array to demonstrate the homogeneity of the tips. Reproduced from⁵².

More recently, a cantilever-free SPL architecture that can generate 100 nm-scale molecular features using a 2D array of independently actuated probes has been reported.⁵⁸ To physically actuate a probe, local heating is used to thermally expand the elastomeric film beneath a single probe, bringing it into contact with the patterning surface. Not only is this architecture simple and scalable, but it addresses fundamental limitations of 2D SPL by allowing one to compensate for unavoidable imperfections in the system. This cantilever-free dot-matrix nanoprinting will enable the construction of surfaces with chemical functionality that is tuned across the nano- and macroscales.

In the latest DPN development called beam pen lithography, an array of tips adds photosensitive material to the surface followed by exposure of the material through a hole in the tip.⁵⁹ Although nanoscale features have not yet been achieved one could envisage combining this method with near-field photolithography in order to create nanoscale three-dimensional structures.

Dip-pen nanolithography has been widely applied to deposit biological material on a sub-cellular scale. The absence of high temperatures and aggressive chemicals make dip-pen nanolithography an excellent tool for sensitive biological materials such as proteins, peptides, DNA, lipids, viruses, and enzymes. As an example

Curran *et al*⁶⁰ reported dip-pen nanolithography deposition for sub-cellular surface modification in stem cell growth by depositing arrays of 70 nm dots with varying pitch (See FIG. 6 (a)-(c)). The dots contained self-assembled monolayers (SAMs) with -OH, -CH₃, -CO₂H, or -NH₂ termination in order to control the initial stem cell attachment and subsequent cell signalling. In this case dip-pen nanolithography provided a method to rapidly scan for stem cell growth factors by large-area nanoscale surface-modification, which is difficult to achieve by other fabrication technologies. Sekula *et al*⁶¹ showed that dip-pen nanolithography can be used to deposit phospholipids containing various amounts of biotin and/or nitrilotriacetic acid functional groups with a 200 nm resolution. The structures were selectively functionalized and subsequently used for selective adhesion and activation of T-cells (See FIG. 6 (d), (e)). One benefit of using ANM is the ability to add functionality to existing structures. This was shown by Mitsakakis *et al*⁶² by using dip-pen nanolithography to deposit lipids with different functionalized head groups on a micro-fluidic surface acoustic wave biosensor. By using dip-pen lithography the sample preparation time was reduced and the sensitivity of the biosensor was increased 5 times. It is beyond the scope of this article to give an exhaustive review of all the biomaterials deposited by dip-pen nanolithography but an overview can be found in two excellent reviews by Zhou *et al*⁶³ and Wu *et al*.⁶⁴

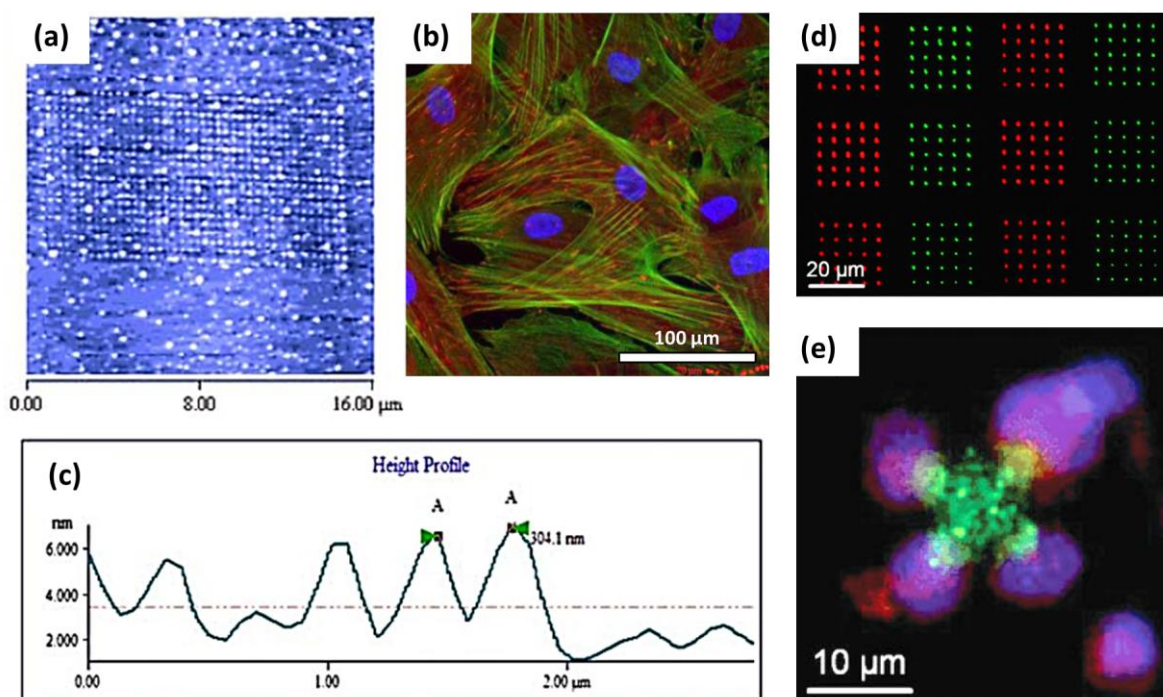


FIG. 6 (a) AFM image of self-assembled monolayer dots printed using dip-pen nanolithography. (b) Human stem cells grown on nanopatterned surface. (c) Height profile of nanodots of self-assembled monolayers. (d) Fluorescence micrograph of phospholipid nanodots patterned by dip-pen nanolithography. (e) Fluorescence micrograph of a T-cell selectively adhered to and activated by functional proteins (anti-CD3/anti-CD28 antibodies) bound to phospholipid multilayer patterns via streptavidin. (a)-(c) reproduced from⁶⁰. (d),(e) reproduced from⁶¹.

DPN has evolved in order to achieve unlimited pattern design, low-cost, high throughput and pattern flexibility. The advances have been rapid and span many fields. However, issues such as individual tip actuation over large areas, feature size reduction to the single-molecule level (for example, individual proteins), and translation of the tips over large distances must be addressed to achieve the full potential of this technology. The use of these techniques as tools for rapid and parallel site-specific chemical transformations is an emerging approach that could transform the manufacturing of gene chips by providing a route to site-specific combinatorial synthesis. **Rapid advances in tip engineering to reduce wear have been particularly important.**^{65,}

66, 67, 68

2.2 Electrohydrodynamic Jet Printing

Inkjet printing by piezoelectric actuation is well known from home printing of documents and photos. The same technology with a little modification has been used to print microscale structures of a wide variety of

materials including proteins,⁶⁹ polymers¹⁴ and nanoparticles.⁷⁰ An alternative driving force to expel the “ink” known as electrohydrodynamic (EHD) jet printing utilizes an electric potential applied between the nozzle and the substrate. The electric potential causes mobile ions to accumulate near the mouth of the nozzle and due to ionic electrostatic repulsion the meniscus deforms into a cone known as the Taylor cone¹⁶ consisting of one or more coaxial liquids (see FIG. 7). At low electric fields the meniscus enters a pulsating mode in which the Taylor cone contracts after expelling each droplet. The frequency of this pulsation is in the kHz range leading to a rapid stream of droplets before the meniscus retracts to its original shape. The time it takes to form a new burst of droplets depends on the flow rate of the supplied solution and the characteristic charging time determined by the resistance and capacitance of the system. If the electric field is increased the Taylor cone stabilizes and a continuous flow is established known as the stable jet mode which is used in electrospinning. At even higher electric fields, multiple jets can form and eventually the atomization mode is reached (also known as electrospraying) in which a fine cloud of droplets is created, a method widely used in mass spectroscopy and for thin film deposition. Thus, EHD jet printing can be harnessed to directly write structures in two or three dimensions or apply thin films with great uniformity. The key advantage of EHD jet printing over other dispensing technologies is that by controlling the electric field strength droplets or liquid streams with a diameter much smaller than the nozzle size can be achieved.^{71, 72} Nozzle clogging is exacerbated by a reduction in the nozzle orifice and is one of the main causes of dispensing failure. Clogging in addition to the difficulties of nanoscale nozzle fabrication are some of the main challenges in any nanoscale dispensing technology.

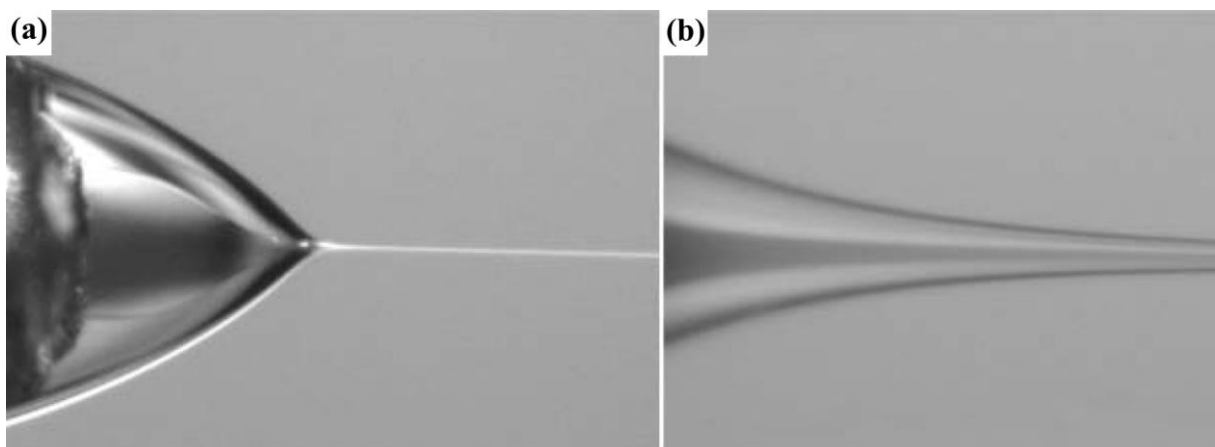


FIG. 7 (a) Photograph of compound Taylor cone containing coaxial fluid flow. (b) Close-up of coaxial jet. Reproduced from⁷².

Through the pulsating mode Park *et al*¹⁶ were the first to show that EHD jet printing can achieve feature sizes below 250 nm by using nozzles with an internal diameter down to 300 nm and reducing the nozzle to sample distance to 100 micrometres. By coating the nozzle opening in a hydrophobic self-assembled monolayer clogging and erratic dispensing was avoided enabling high quality printing. Through an integrated computer-controlled system the group showed printing of complex structures in both conducting and insulating polymers as well as solutions of silicon nanoparticles and rods and single wall carbon nanotubes. They were also able to show printing of interconnects and functional transistors with critical dimensions down to 1 μm on a flexible plastic substrate.

EHD jet printing was taken even further by Galliker *et al*⁷³ who improved the resolution and extended the technology into the third dimension through electric field enhancement and rapid solvent evaporation. The resolution was improved by reducing the substrate to nozzle distance to 3-4 μm which enabled structures down to 50 nm to be written (see FIG. 8). The electric field enhancement from the first droplet guides the second droplet to land in exactly the same spot. In this way vertical and tilted gold nanowires with a 50 nm diameter and 850 nm heights could be fabricated (see FIG. 8 (d)).

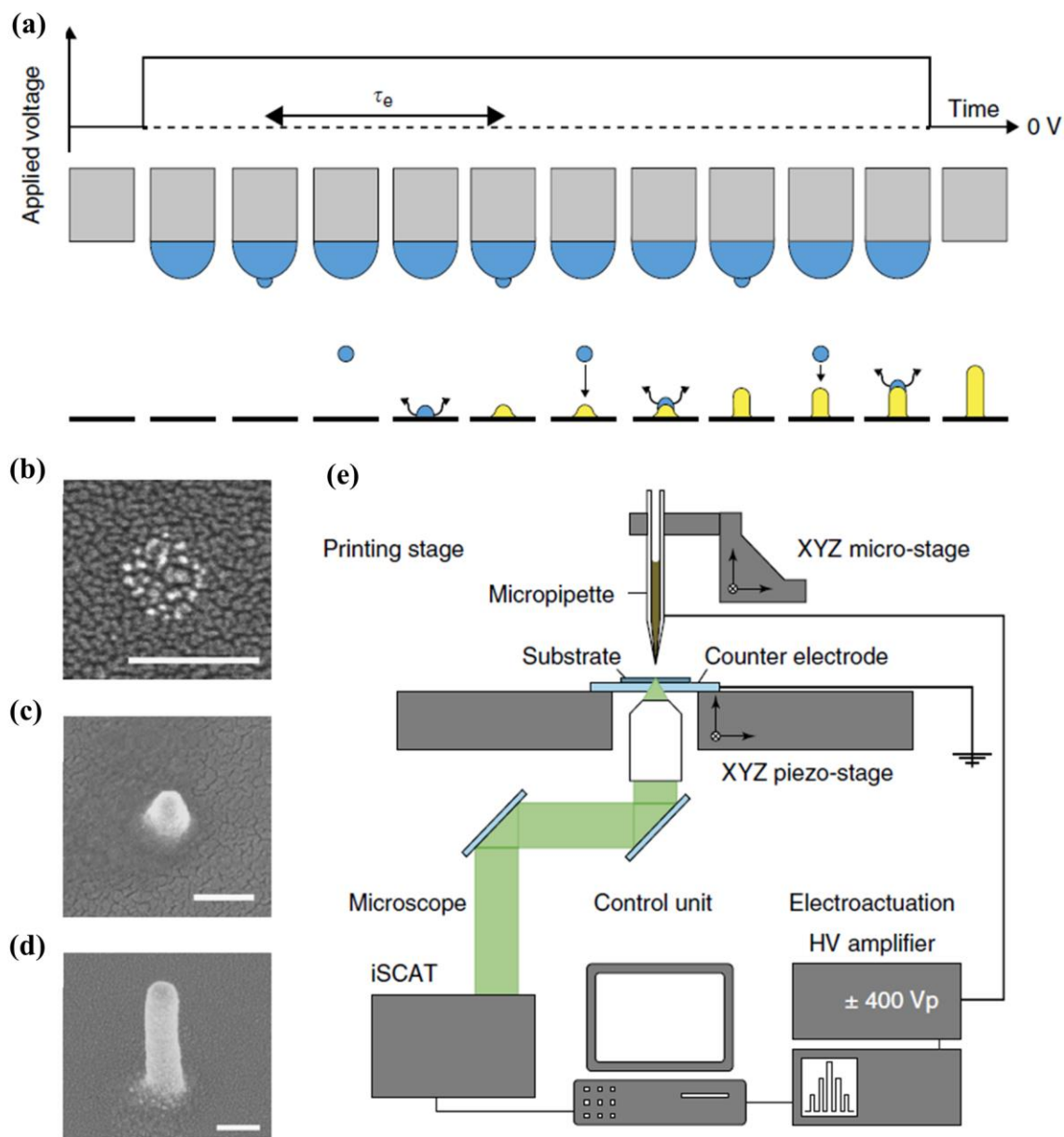


FIG. 8 Schematic of EHD printing process and set-up. (a) Growth of a liquid meniscus and subsequent ejection of ink nanodroplets from its apex on application of a DC voltage. During DC on-time, droplets are ejected at a homogeneous period τ_e and, once impacted, are vapourized (represented by wavy arrows) in the course of τ_e . After periodic repetition of this event (for illustration convenience merged into one cycle), a sharp structure consisting of a multitude of formerly dispersed nanoparticles rises from the substrate, attracting approaching charged droplets by electrostatic nanodroplet autofocussing (straight arrows). The growth process is further illustrated with SEM micrographs (150 nm scale bar) of (b) the deposition pattern of a single nanodroplet and that of (c,d) actual nanopillars. (e) Schematic of the ENA NanoDrip set-up with the nozzle located above an underlying glass substrate placed on an ITO-coated glass slide representing the grounded counter electrode. Voltage stimuli were applied in the form of amplified DC signals between the ink-filled, metal-coated pipette and the counter electrode. Reproduce from⁷³.

The nonlinear relationship between the applied voltage and droplet diameter was shown experimentally to vary the droplet diameter from the size of the nozzle orifice (1.2 μm) down to 80 nm at which point further

electric field increments had no effect on the droplet diameter. This 15x reduction in feature size helps **preventing** clogging and enables microstructures to be written with the same nozzle as nanostructures. The applied voltage also increases the frequency with which the droplets are expelled (up to ≈ 100 kHz) and thereby the flow rate of the dispensed solvent. The increased frequency was shown to be outweighed by the reduction in droplet diameter thereby reducing the overall flow rate by almost a factor 100. However, near the minimum droplet diameter the flow rate reaches a minimum and further increase in applied voltage was able to restore the flow rate to near its original value ($\approx 100 \mu\text{m}^3/\text{s}$). The implications of this is that with the given nozzle size, 80 nm wide lines can be written faster than 1 μm wide lines. Such inverse scaling of throughput to feature size is in contrast to other techniques and can thus be advantageous for nanomanufacturing.

Combining EHD jet printing with block-copolymer self-assembly provides a pathway for further reduction in minimum feature size. The flexibility of EHD jet printing allows a desirable mixing of block-copolymers with different molecular weight and the material waste of the relatively expensive polymers is greatly reduced. In this way periodic structures with length scales ranging from centimetres to ≈ 10 nm can be fabricated⁷⁴ within the geometrical limitations of block-copolymer self-assembly.

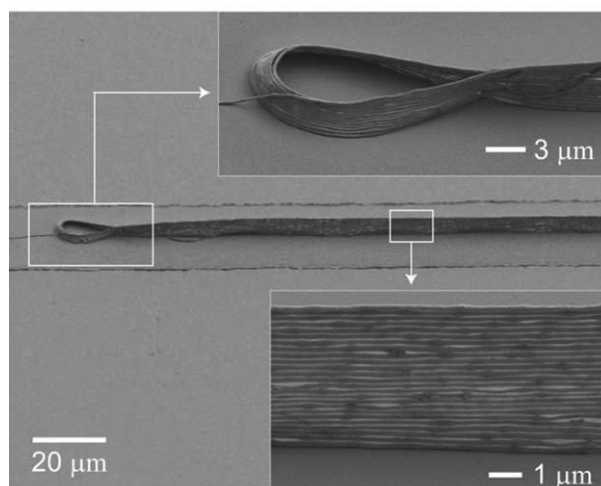


FIG. 9 Poly(ethylene oxide) three-dimensional structures fabricated by electrospinning. Reproduced from⁷⁵.

Electrospinning from the stable jet mode is used for fast deposition of organic and polymer fibres for applications in nanowire electronic devices, physical biomimetic structures, and field-effect transistors. Traditional electrospinning can form fibres with speeds up to 10 m/s but the fibres are unaligned and form a mat of cross-linked fibres because of an uncontrollable wiping motion of the forming fibre.⁷⁶ By reducing the distance between the nozzle and the substrate straight fibre arrays can be formed.^{77, 78} Through a further

reduction of the distance and the applied voltage the fibre diameter can be reduced to 50 nm and positioned with great accuracy.⁷⁹ A further development known as mechano-electrospinning utilizes the drawing force on the fibre from the moving stage to stretch the fibre⁸⁰ achieving well-organized arrays of sub-20 nm diameter fibres.⁷⁹ The fibre diameter decreases with the drawing speed and could be drawn with up to 40 mm/s. Recently Lee *et al*⁷⁵ extended electrospinning to the third dimension by utilizing the electric field enhancement from a Pt electrode to control the wiping motion. By repeatedly passing the fibre along the same path 180 nm wide and 4.5 μm tall walls of poly(ethylene oxide) were deposited (see FIG. 9). Additional advantages of electrospinning is the ability to fabricate hollow,⁸¹ co-axial⁸² and mixed composition nanowires⁸³ in one step. An impressive example of the materials and dimensions achievable by electrospinning was reported by Nuansing *et al*⁸⁴ who were able to deposit peptide and protein nanowires with a diameter around 100 nm but on occasion down to 5 nm, corresponding to a single molecule (see FIG. 10). These fibres will be highly biocompatible and biodegradable and a potential candidate for the most critical biological and medical applications, such as the proliferation of stem cells. Although these nanofibres were randomly orientated, the recent advances within EHD Jet printing mentioned previously in this review would enable controlled deposition.

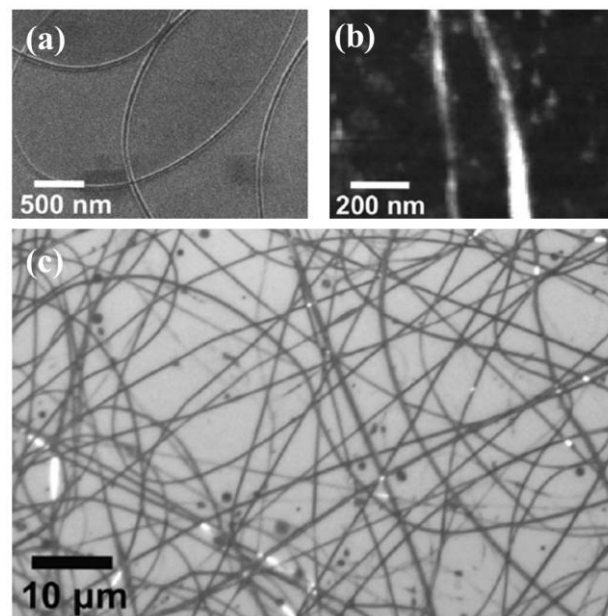


FIG. 10 (a)-(c) Biocompatible albumin (protein) nanofibres with diameters below 100 nm fabricated by electrospinning. Reproduced from⁸⁴.

Electrospraying (electrohydrodynamic spraying) is a method closely related to electrohydrodynamic direct writing in that an electric potential is applied between the nozzle and the sample to draw the solution

containing charged particles from the nozzle. The distinction of this technique with regards to the pulsating and stable jet mode is that the electric field is much higher in this technique. In electro spraying the repulsive forces from the charged particles overcome the surface tension of the expelled liquid thereby breaking up the solution into droplets. Potential evaporation of the solution increases the repulsive surface charges thereby further breaking up the droplet into a cloud of micro- or nanodroplets.⁸⁵ The size of virtually monodisperse droplets can be controlled by the solution flow rate, electrical potential at the nozzle, and nozzle diameter. Because the droplets are electrically charged, coagulation is absent. The trajectory and focus of the charged particle beam can also be controlled by an external electric field.⁸⁶ In this way Lee *et al* were able to focus electro sprayed silver nanoparticles to write lines 100 μm wide and 100 nm thick with a deposition rate of 2 $\mu\text{L}/\text{min}$.⁸⁷

Electro spraying is a flexible deposition method that has been used for thin film deposition, direct writing, and nanoparticle fabrication within a variety of fields. Virtually all materials can be electro sprayed, which means that organic as well as inorganic thin films can be formed. An excellent review paper by Jaworek *et al*⁸⁶ lists more than 40 materials and their solvents that have been used so far. Due to the spraying nature of the process the resolution of the process is currently limited to 100 μm for direct writing. Therefore electro spraying is not suited for direct writing of nanostructures but can distribute nanoparticles locally. However, electro spraying is a mature technology with a wide range of proven material choices which for the most can be used for nanofabrication if operating in the pulsating or stable jet mode EHD jet printing. A search for materials to use in EHD jet printing can hereby benefit from looking through the literature for electro spraying.

Taking into account the high writing speeds, wide material choice, and ability to print in three dimensions, the possibilities for EHD jet printing are vast. However, because EHD jet printing does not have an inbuilt alignment technique, as is the case for manufacturing technologies based on microscopy techniques, aligning consecutive layers will prove more difficult. Nevertheless, this technology is one of the most promising ANM technologies for large-scale fabrication of structures where nanoscale alignment is not essential.

2.3 Direct Laser Writing and Resist Based Nanomanufacturing

Direct laser writing (DLW) of nanoscale features is capable of building 3D structures from the ground up in a rapid and facile manner (see FIG. 11). Although DLW is a resist based fabrication method and therefore requires an additional development step, it is very similar in nature to additive nanofabrication because the fabricated structures have their final shape without following deposition or etch steps. Laser driven three-dimensional (3D) nanofabrication ~~this~~ is best achieved by multi-photon polymerisation (MPP).^{88, 89} In MPP, the concentration of photons in the neck of a femtosecond pulse of a laser beam allows for the controlled photopolymerisation of a targeted volume (or voxel) in a photoresist. Development of this resin allows 3D features to be written at typically 10 to 500 $\mu\text{m/s}$ with nanoscale resolution. This is particularly useful for fabricating 3D photonic structures^{89, 90, 91} that would otherwise be extremely expensive and difficult to manufacture with the alignment of sequential 2D layers via traditional lithography. The successful commercialisation of this technology by companies like Nanoscribe GmbH has enabled photonics researchers to investigate new applications in 3D with invisibility cloaks^{90, 91}, Gecko-mimicking surfaces⁹² and 3D data storage⁹³ among other impressive achievements in recent years.

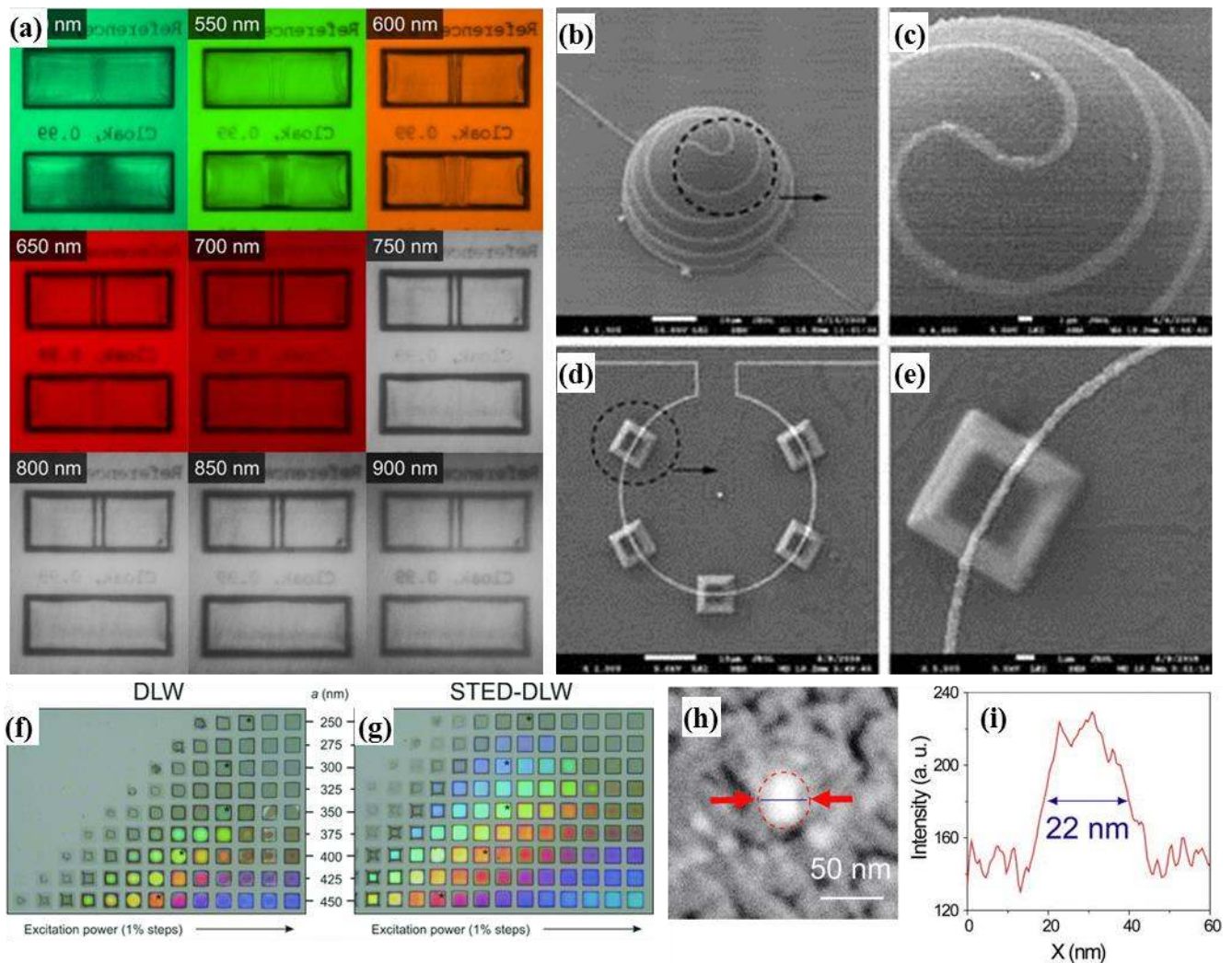


FIG. 11 Features and devices created by Direct Laser Writing literature (a) True colour images of carpet invisibility cloak for unpolarised light, ranging in wavelength from 500 to 900 nm, with both reference and cloak structures. Reproduced from⁹¹. (b-e) SEM images of silver microscale lines drawn arbitrarily onto 3D structures. Reproduced from⁹⁴. (f, g) True-colour reflection-mode optical micrographs of woodpile photonic crystals $20 \times 20 \mu\text{m}^2$ fabricated by (f) regular DLW (MPP) and (g) STED-DLW. Reproduced from⁹⁵. (h) SEM image of a 22 nm silver dot grown by laser driven nucleation and growth, with (i) the corresponding intensity profile as indicated in the micrograph. Reproduced from⁹⁶.

The range of materials that can be polymerised for MPP nanofabrication is a significant challenge for materials science to explore. For solid structures advanced composites or solutions that respond to MPP have been demonstrated, resulting in structures of vanadium⁹⁷ and silver⁹⁶. The simplest approach to avoiding this is to use the surfaces of 3D polymer structures as scaffolds for the deposition of other materials. Metallisation of such scaffolds by atomic layer deposition or electroless plating has been shown to work for metallic photonic crystals⁹⁸ and metamaterials.⁹⁹ The polymer structures written can also be used for casting of 3D structures from other materials like titania.¹⁰⁰

Maximising the resolution of MPP is of course an important goal, with Abbe's diffraction limit representing the typical limit. A recent review¹⁰¹ summarised the advances in sub-diffraction limit DLW. As an example Cao *et al* achieved the highest resolution of this technique to date with 40 nm dots in a highly sensitive photoresin¹⁰² and 22 nm silver dots by laser activated nanoparticle growth.⁹⁶ These results are extremely impressive, but the high resolution was only achievable for individual dots. When continuous structures were attempted, a larger line width of 130 nm was achieved at a comparatively low scanning speed of 3 $\mu\text{m/s}$.¹⁰² Stimulated emission depletion (STED), which has achieved 5.8 \pm 0.8 nm resolution in microscopy,¹⁰³ is also being put forward as a promising route to sub-diffraction MPP. It has been effective in building 3D nanoscale structures over a large area^{91, 100} and shows significant improvement over regular MPP for 175 nm parallel structures⁹⁵ achieving 65 nm line widths¹⁰⁴ whilst scanning at 100 $\mu\text{m/s}$.

DLW is also able to create a wider range of features in 2D by initiating reactions locally with the input of energy from the laser. This includes reducing graphite oxide to draw supercapacitors,¹⁰⁵ the laser-induced chemical vapour deposition of graphene on Ni,¹⁰⁶ the growth of carbon nanotubes,^{107, 108} and the electroless plating of silver.⁹⁴ Integrating these technologies could enable the entirely laser driven fabrication of carbon nanotechnologies. Other methods of laser writing like sintering of a silver nanoparticle ink¹⁰⁹ could work well for large scale patterning of electrodes. In these cases higher scan speeds up to 1000 $\mu\text{m/s}$ have been shown to reduce the features line width and height to below 5 μm and 50 nm respectively, with an increasingly high surface roughness an unfortunate consequence.

Although technically not an additive manufacturing method, scanning near-field photolithography provides a cheap alternative to traditional nanoscale photolithography. By utilizing the evanescent field from an illuminated nanoscale aperture in close proximity to the photoresist, direct writing of sub-diffraction limited structures with resolution down to 70 nm can be achieved.^{110, 111, 112} Vast improvements to this technology has been achieved by utilizing flying plasmonic lenses thereby potentially outperforming electron beam lithography in terms of cost and speed.¹¹³ The inventors envisage this technology to be able to pattern a 12 inch wafer in 2 min with sub-100 nm resolution in the future.

3. Single Particle Placement

Single particle placement covers both the ability to create structures atom-by-atom and positioning pre-prepared nanoscale objects within an existing framework. We will cover electrical, mechanical and optical methods to attract, retain, and position particles enabling fabrication of the smallest human-made structures. We will especially focus on the possibilities afforded by Scanning Probe Microscopy (SPM) technologies, electrokinetics, and optical confinement. ~~Finally we will briefly cover some of the possibilities self-assembly offers including the prospect of combining self-assembly with other single particle placement methods.~~

3.1. Building Atom-by-Atom ~~using STM~~

~~Building devices from individual atoms remains the ultimate long-term goal for researchers in nanotechnology. As of yet, the only machines proven capable of such manipulations are SPM technologies: the scanning tunneling microscope (STM) and the atomic force microscope (AFM).~~

In arguably the most well-known use of a STM, researchers at IBM pioneered atomic manipulation by rearranging Xe atoms on a Ni substrate to spell out "IBM" (FIG. 12 (a) and (b)).¹¹⁴ ~~AFM manipulation of atoms even advanced the technology up to room temperatures, achieving the atomic switching of adatoms¹¹⁵ (see FIG. 12(c)-(e)) or the more unconventional vertical interchange of atoms between the surface and the tip.¹¹⁶~~ ~~These approaches demonstrate the~~ impressive atomic limit of the current technology and ~~are~~ used frequently in fundamental research to position and characterise atoms and molecules.^{117, 118, 119} Although STM probes do not offer high throughput, it is the most precise nanomanufacturing tool available and is being used to fabricate some of the first single atom transistors for quantum computing.¹²⁰ The process known as STM lithography involves selectively driving the electrical desorption of hydrogen atoms from the surface of hydrogen passivated silicon and letting a phosphorus atom diffuse through the window formed by the missing hydrogen atom.

~~The manipulation methods of nanoscale objects by STM have been improved by the combination of multiple STM probes with scanning electron microscope (SEM) imaging allowing simultaneous visual guidance with manipulation and electrical characterisation of atomic to nanoscale devices.¹²¹ The consolidation of these functions has been useful to researchers, who can take measurements and images of their devices during processes driven by the probe tips. For example in work by Qin *et al*,¹²⁴ this is demonstrated with carbon~~

fibres that are pushed, bent, burnt and broken under the real time observations of the SEM (see FIG. 13 (a) and (b)). Unfortunately, the need for active engagement of a human operator with the machine to ensure the success of iterative manipulation steps makes industrial adaptation impractical at present, with the best applications available in pure research.

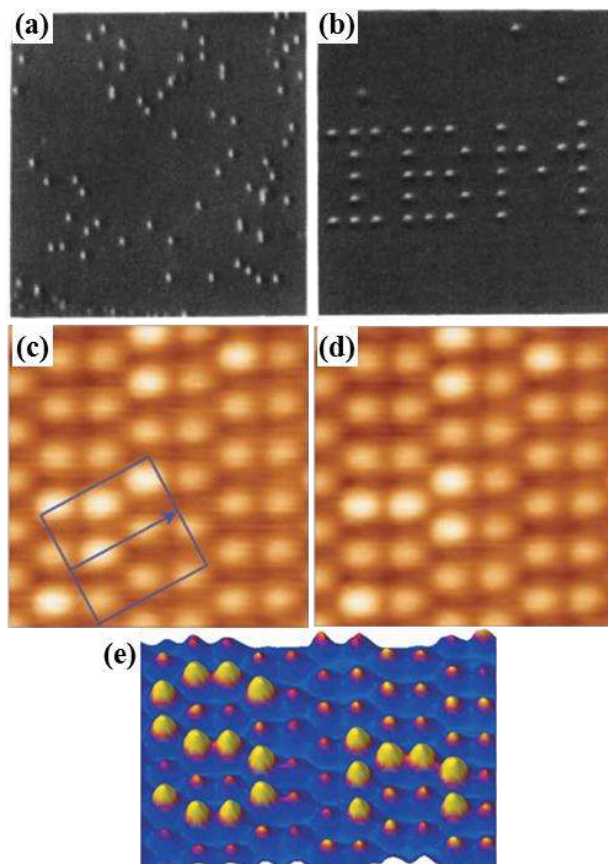


FIG. 12 (a, b) STM images of the arrangement of Xe atoms on a Ni surface (a) before and (b) after manipulation with the STM probe. Reproduced from¹¹⁴. Each letter is 5 nm from top to bottom. (c-e) A sequence of AFM images showing the lateral manipulation of substitutional Sn adatoms in a Ge surface by inducing adatom exchange at room temperature with an AFM probe tip. Reproduced from¹¹⁵. One of these manipulation steps is presented (c) before and (d) after adatom exchange of the brighter Sn atoms and (e) shows the final AFM image of the Sn atoms rearranged to give the atomic symbol Sn. (c) and (d) are $4.6 \times 4.6 \text{ nm}^2$ and (e) is $7.7 \times 7.7 \text{ nm}^2$.

3.2. Nanoparticle Manipulation by AFM

The visual image of additive manufacturing is often a robotic arm picking up a component and inserting it into another component. This literal understanding of AM has been miniaturized and microscale electrothermally actuated robotic arms have been used to break off vertically aligned carbon nanotubes and place them onto surfaces, such as on the tip of an AFM probe.^{122, 123} With arms like these even nanotubes tens of nanometres

in diameter can be gripped and moved.¹²⁴ Although this is a process that struggles to manipulate smaller nano-objects and operates at temperatures too high for many applications, microgrippers challenged the idea that some objects are just too small to pick up and place in a desired location.

The AFM offers more flexibility to researchers; it is capable of manoeuvring a diverse range of materials from nanoparticles^{125, 126} and atoms^{115, 116} to biological cells,¹²⁷ be it under vacuum or immersed in liquid. The rudimentary method of nanoparticle manipulation with an AFM uses the probe tip to push, pull and slide nanoparticles around on a substrate, positioning them into desired configurations.¹²⁸ By moving the probe on a vector through the centre of the targeted particle in the desired direction, the nanoparticle can be moved across the surface by the interaction forces between the nanoparticle and tip apex. Unfortunately these methods have very low throughput and require the operator to constantly image the surface to track the particle's progress. The accuracy of each iterative process has a high uncertainty, since the particle will be likely skewed to one side or the other of the intended path if not pushed *precisely* in the centre, which becomes more likely for smaller particles. Recognising these flaws, Kim *et al* pioneered a novel method of manipulating nanoparticles whilst simultaneously imaging the surface.¹²⁵ They relied on the principle that static friction is time-dependant and will increase if two surfaces are left inert. They studied 15 nm Au nanoparticles on planar quartz surfaces. One nanoparticle was initially "kicked" to reduce the standing friction, before the surface was scanned at a sufficiently high rate (~7Hz) with the AFM in tapping mode. The kicked particle moved across the surface in a direction perpendicular to the scanning axis, with motion ceasing abruptly and precisely when the scan speed was dropped below the threshold. This phenomenon resulted from the mechanical force the probe tip exerts on the nanoparticle on each pass pushing it along the surface, which also created ghost images of the particle giving an intuitive picture of its path. Critically, this result was only observed for the nanoparticle that was initially kicked, validating the hypothesis regarding the importance of the change in friction. To demonstrate how effective this technique was, they ran comparison studies with the existing manipulation method, reporting that efficiency was improved by a factor of 5 to 10 whilst achieving at least parity of precision. Using this method of nanomanipulation, the same group have managed to characterise the coupling between a gold nanoparticle in a hybrid nanostructure with a semiconductor

quantum dot,¹²⁶ demonstrating the usefulness of this technique to more efficient mechanical manipulation. Testing with other particles and nanoscale objects will be needed to see how transferrable the method can be.

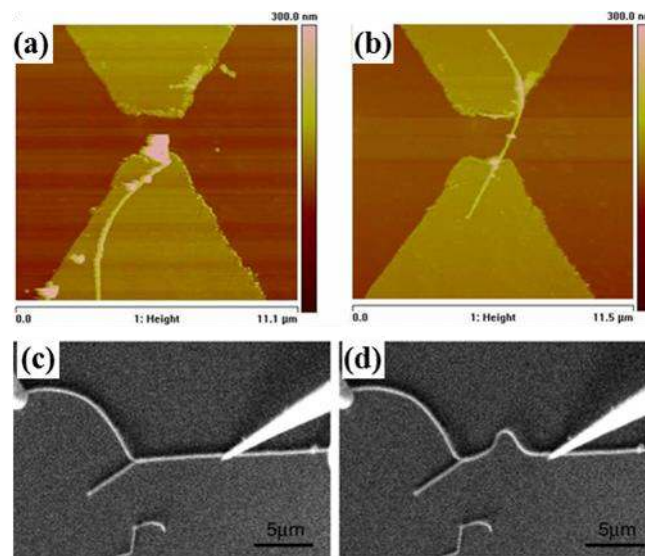


FIG. 13 (a, b) An AFM probe with a haptic force feedback is used to move a carbon nanotube on the surface between two electrodes to create an infrared sensor. Reproduced from¹²⁹. **AFM images (a) before and (b) after the nanomanipulation show the successful transfer. (c, d) SEM images of the bending of a carbon nanofiber with an STM probe in a 4-probe STM system. Reproduced from¹³⁰.**

In an alternative approach to circumventing the unreliable manipulation of objects with the AFM, Li *et al* have developed a system that generates real-time force feedback to the operator through a haptic joystick,¹³¹ that is also used to update AFM scans of the surface.¹³² The development of this technology¹³³ has culminated in a corrective fabrication technique, wherein carbon nanotubes (CNTs) are assembled near electrodes by dielectrophoresis before being repositioned to bridge the electrode gap (see FIG. 13 (a) and (b)).¹²⁹ Using this technique of nanorobotic manipulation, they were able to build and test single-walled, multi-walled and bundles of CNTs onto electrodes to operate as functional infrared sensors.

In many cases, visualisation is realised by building the manipulators into an SEM setup to give operators real-time visualisation of the objects they are controlling. This is a common combination for microgrippers, but has also been employed using SPM probes. For example, in work by Qin *et al*¹³⁰, carbon fibres are pushed, bent, burnt and broken under the real-time observations of the SEM (see FIG. 13 (c) and (d)). The combination of these machines could prove useful to researchers, who can take measurements and images of their devices during processes driven by the probe tips.

The need for active engagement of a human operator with these different mechanisms to ensure successful manipulation of nano-objects makes industrial adaptation impractical at present, with the best applications available in pure research. This problem may be solved if recognition and positioning of components can be automated by software. Additionally, mechanical manipulations are primarily limited to the 2D rearrangement of existing nano-objects, which limits the scope for 3D manufacturing.

3.3 Electrokinetic Nanomanipulation

A force can be exerted on charged objects in solution when in a DC electric field, an effect known as electrophoresis, which allows for straightforward manipulation of particles towards charged surfaces. These charged surfaces are easily created by the application of a DC voltage between electrodes,¹³⁴ although alternative methods of charge patterning down to hundreds of nanometres can also be used to direct the 2D assembly of components.^{135, 136, 137} Electrophoresis has been criticised for being limited to the manipulation of charged objects. However, the ability to functionalise nanoparticles with surface monolayers¹³⁸ enables a wide variety of nanoparticles to be manipulated. It should be noted, though, that some researchers have encountered problems when attempting to assemble films with DC or AC fields alone.¹³⁹

Analogously, dielectrophoresis refers to the force generated on a neutral particle when it is in an AC electric field: the electric field polarizes the particle, which in the non-uniform field results in a non-zero Coulomb force acting on the particle. Although two electrodes are usually required for dielectrophoresis¹⁴⁰, the use of a triaxial probe to generate a dielectrophoresis field that acts as a non-contact trap for dielectric nanoparticles has been recently demonstrated^{141, 142} (see FIG. 14). This method is proposed to work for particles as small as 5 nm¹⁴¹ and has been verified for the isolation of 100 nm polystyrene beads.¹⁴² The non-contact manipulation of nanoparticles in 3D can thus be achieved, with the probe moving the particle through the solution and releasing it on command. However, the strength of the trap limits the positioning accuracy of the particles in the solution, with the polystyrene beads having standard deviations of 133 nm and 204 nm in the x and y axes from the intended location. The increasingly strong influence of Brownian forces will only exacerbate this problem as the manipulated particles become smaller. However, if the electric field confining the particle

could be amplified, then its position might be more easily confined, and the accuracy improved. Despite the initial problems, this method represents one of the most impressive results within nanoparticle manipulation.

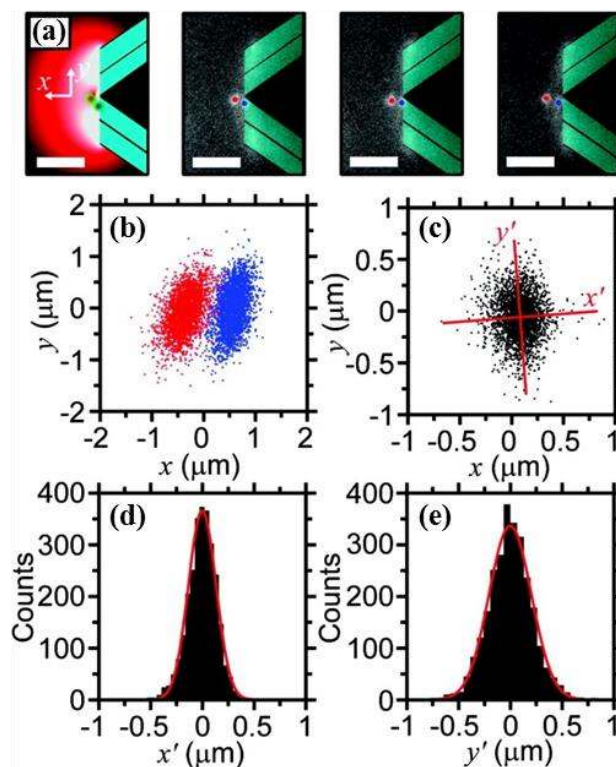


FIG. 14 Non-contact capture of 200 nm polystyrene beads by a triaxial probe by dielectrophoresis. Reproduced from¹⁴². (a) Schematic and three representative fluorescence images of a 100 nm radius bead trapped in the negative-dielectrophoresis trap. (b) Scatter plots of the position of the bead in the trap (red dot) and the tip inferred from the position of an attached bead (blue dot). (c) Scatter plot of the separation between the trapped bead and the triaxial tip given by the separation of trapped bead/adhered bead pairs. The axes of tightest and loosest trapping are determined with principle component analysis and are shown on the plot as the x-axis and y-axis respectively. (d) Histogram of the spread of the trapped bead about the x-axis. (e) Histogram of the spread of the trapped bead about the y-axis.

3.4 Optical Nanomanipulation

The energy profile of a laser can be used as an optical trap for metallic and dielectric nanoparticles, capable of 3D manipulation. The forces exerted by these *optical tweezers* are only of the order of piconewtons, generally making it useful only for objects immersed in liquid media, which has seen it used primarily for manipulating biological entities.¹⁴³ Recent advances are now allowing the manipulation of nanoscale objects,^{144, 145, 146, 147} like gold nanoparticles¹⁴⁵ and silver nanowires¹⁴⁷ arbitrarily positioned onto surfaces. The error in the positioning of these particles, however, was untenably high for reliable fabrication practices e.g. 40 nm particles with deposition errors on the order of hundreds of nanometres.¹⁴⁵ This limitation to the tweezers is unfortunate,

given the flexibility of manipulation it offers such as using the polarisation of the light to orient and align the objects.^{144, 146}

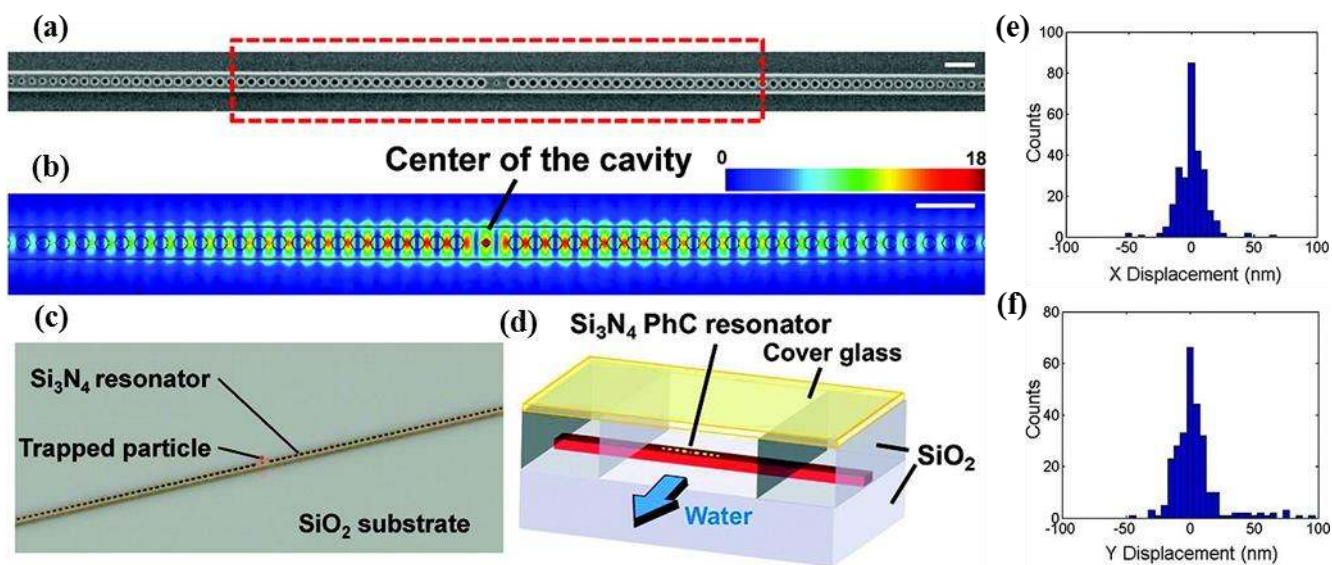


FIG. 15 The capture of 22 nm polymer nanoparticles in a photonic crystal (PhC) resonator. Reproduced from¹⁴⁸ (a) Scanning electron microscope image of a silicon nitride PhC resonator. (b) FDTD simulation showing the electric field distribution near the resonator cavity (indicated by the red dashed lines in panel (a)). The colours indicate the relative field intensity (arbitrary unit). Strong field enhancement can be seen within the small hole at the centre of the cavity. Scale bars in (a) and (b), 1 μm . (c) Schematic showing trapping of a nanoparticle on a silicon nitride PhC resonator. (d) Schematic showing the relative locations of the resonator and the flow chamber. The resonator and the waveguides connected to the resonator are on the top of a silicon dioxide layer. The upper part of the resonator is exposed to the aqueous solution in the flow chamber, while the waveguides connected to the resonator are surrounded by silicon dioxide. (e, f) Histograms of the displacement of the trapped particle from the trap centre in the X and Y direction.

The precision of this placement can be improved though: for instance by coupling the laser with cavities in an optical resonator, it has been demonstrated that even 22 nm polymer particles can be immobilised in the cavities¹⁴⁸ (see FIG. 15). Because these cavities increase the electric field density within them when the laser is on, with positioning error typically within 25 nm achieved. This is comparable to the accuracy of the self-assembly approach to single-particle placement.¹⁴⁹ The use of these nanoapertures also benefits from a low increase in temperature of approximately 0.3 K, which helps limit the attraction of multiple particles to the aperture by thermophoresis and avoids damaging biological entities during manipulation. Following a similar design practice 50 nm polystyrene beads have recently been trapped in a nanoaperture on an optical fibre and manipulated in suspension over several microns¹⁵⁰ (See FIG. 16). This near-field optical nanotweezer is able to both manipulate and track the particle in 3D through the same fibre, allowing a facile means of manipulating dielectric nano-objects, even though the wavelength of the laser used was more than 21 times the diameter of the bead. Additionally, the reflected signal collected by the fibre was able to make a distinction as to whether or not a particle was currently trapped at the tip. This represents an important leap forward into the nanoscale world for optical tweezers, almost certainly establishing the use of similar apertures for future mechanisms.

The plasmonic heating effect can nevertheless be put to good use: by exposing a gold nanoparticle embedded in a layer of PDMS to laser light, the localised heating cures the PDMS in proximity to the particle.¹⁵¹ The laser also acted as an optical tweezer, which was able to move the particle around to draw 2D features into the PDMS, with no curing of the PDMS observed due to laser exposure alone, and producing PDMS nanowires several microns in length and 120-130 nm in diameter. It remains to be seen if these features could then be used as a mask for further processing. There is also a difficulty that arises from continuously write with a nanoparticle without retracing previous paths used by the particle to prevent over-cured and thus over-sized features, to build full nanostructures. Any large scale patterning with multiple particles would also need to initially locate particles in the PDMS, and write structures whilst presumably not coming into proximity of other particles causing unintended curing. However, the potential to write 3D features in this manner is an exciting future area of research.

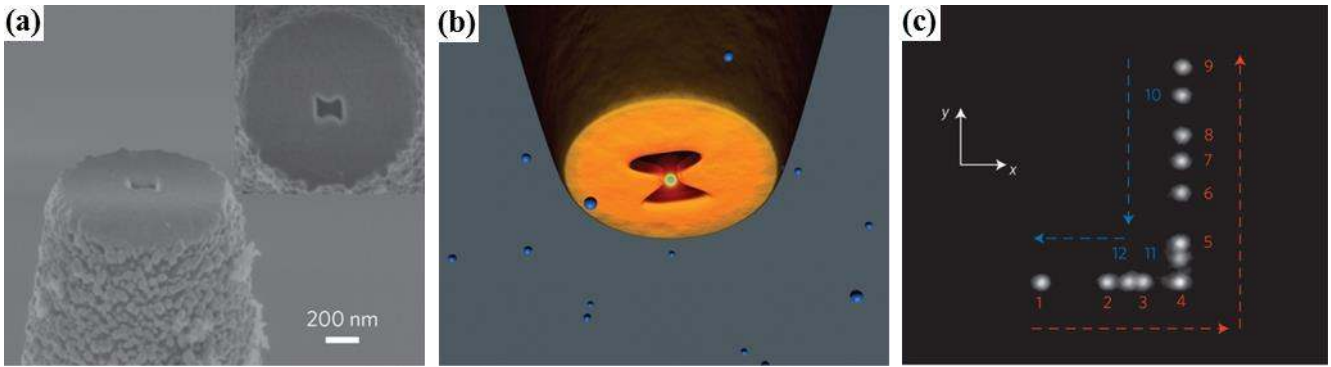


FIG. 16 The capture and manipulation of a 50 nm polystyrene bead with a near-field optical tweezer. Reproduced from¹⁵⁰ (a) SEM image of an 85-nm-gap bowtie nanoaperture patterned at the extremity of a tapered optical fibre. (b) Schematic of experimental configuration. The 1,064 nm trapping laser is directly coupled into the fibre to excite the transverse mode of the bowtie nanoaperture. (c) Composite image reproducing the displacement of the trapped object. This displacement takes place over a 30 s time period with numbers 1–12 represent the successive steps of the tip and particle movement.

3.5 Self-assembly

By exploiting chemical processes through which materials bond to each other, it is possible to self-assemble features from the bottom-up with molecules and particles as the building block. The assembly of these components can be directed by a variety of interparticle forces,¹⁵² which are commonly used to create molecular monolayers on surfaces, which is extremely useful for thin film applications,¹⁵³ and ordered arrays of nanoparticles.¹⁵⁴ This has proven to be an extremely useful tool for nanofabrication, with an extensive body of research investigating the various methods and applications of self-assembly.^{154, 155, 156}

Combining multiple methods of self-assembly has even succeeded in the creation of an operational 3D motor from a single polymer crystal.¹⁵⁷ Successive self-assembly processes allowed a crystal of R-hydroxyl- ω -thiol-terminated polycaprolactone to be coated in three different types of nanoparticles: gold nanoparticles to facilitate optical visualisation; platinum nanoparticles to drive the motor by catalysing the decomposition of the surrounding hydrogen peroxide solution; and iron oxide nanoparticles to allow for remote magnetic guidance of the motor. The functioning motor is shown to perform all of these functions simultaneously, with attempts at moving around magnetic polystyrene microparticles proven partly successful. This type of study shows just how useful nanoparticles and self-assembly are to expanding the functionality of complex devices.

However, the exact positions the molecules bond to in self-assembly requires careful engineering of the devices; lithography methods are vital to ensuring that the assembly occurs in the right locations. Self-

assembly is therefore not available as a standalone fabrication method that can build completely arbitrary assemblies, but it does allow for existing surfaces and objects to be functionalised to perform other useful tasks,^{153, 158, 159, 160} including large-scale growth of features like carbon nanotubes for circuits.¹⁶¹

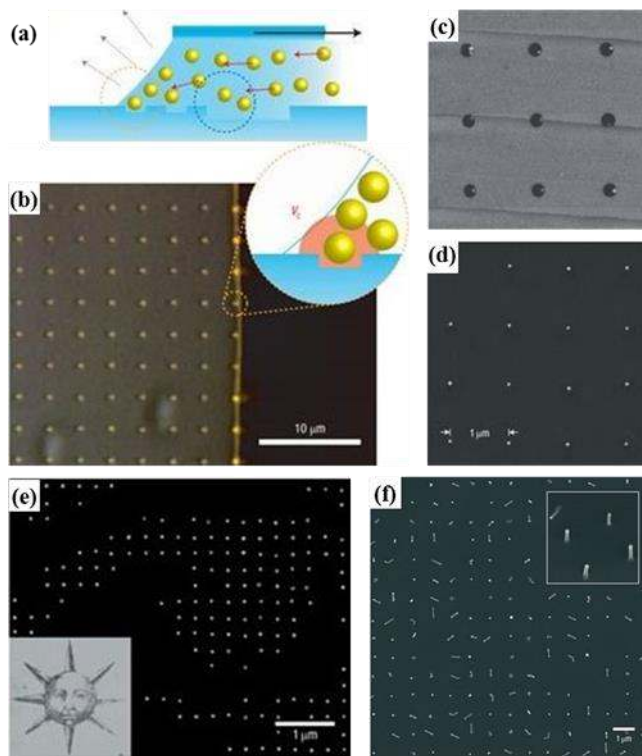


FIG. 17 Single nanoparticle printing. Reproduced from.¹⁶⁰ (a) Schematic of the nanoparticle capture process: a colloidal meniscus containing 60 nm Au nanoparticles is drawn across an indented PDMS surface. (b) A bright-field optical micrograph of the assembly in action; the bright line indicates the accumulation zone of nanoparticles in the colloid. (c, d) AFM topography scans of 60 nm Au nanoparticles (c) captured on the PDMS stamp and (d) printed onto a silicon substrate. (e) SEM image of detail (left eye) from a printed array of Au nanoparticles. (f) SEM image of silicon nanowires grown from a printed array of Au nanoparticles (inset is tilted).

Patterning areas of a surface for self-assembly, although limited to the resolution of the preceding lithography steps, can even direct the very precise manipulation of nanoparticles individually. For instance, 60 nm gold nanoparticles were shown to be isolated onto a PDMS stamp by drawing a meniscus of gold colloid across the indented surface¹⁶⁰ (see FIG. 17). As the nanoparticles that accumulated at the edge of the meniscus pass over the surface indents, individual nanoparticles are drawn into each dent by capillary forces while the Stokes drag of the meniscus pulls additional particles away. Transfer printing was then used to attach these gold particles to a separate PMMA coated substrate, transferring the majority of the pattern and allowing the PDMS stamp to be reused. Once hydrogen plasma cleaning has removed the PMMA film, the nanoparticles were shown to have retained their functionality for nanowire growth. Similar approaches to capillary driven assembly have

also reported the capture of Au nanoparticles down to 2 nm in diameter.¹⁶² Since this technique can be extended to other types of nanoparticles, provided very good accuracy during transfer (reportedly within 100 nm of their captured locations) and a positioning error rate of less than 20 p.p.m., this approach to nanoparticle printing could be extremely useful in nanomanufacturing. It may also benefit from an update with some of the latest transfer printing techniques being developed.¹⁶³

Unfortunately capillary assembly makes it hard to control the exact location that nanoparticles will adhere to, which is very important to positioning particles in desired configurations. A more accurate method of isolating nanoparticles may instead be achieved by electrostatic interactions between a colloid and self-assembled monolayers¹⁴⁹ (See FIG. 18). The proof-of-concept device worked by employing patterned circular areas of a substrate with a self-assembled monolayer (SAM) terminated by amino groups, and the surrounding area with a carboxyl terminated SAM: these two surfaces had a static surface charge in solution (relative to the pH level) as a result of protonation and deprotonation respectively, such that the area inside the circle was positively charged and the area outside was negatively charged. Immersion of this *gate* in 20 nm colloidal gold nanoparticles capped with citrate ions that carry a negative surface charge in solution, resulted in the attraction of the gold towards the *gates'* positively charged area, with the surrounding negative charge funnelling the gold nanoparticles to the centre of the *gates*. Once one of these particles was bound to a gate, the negative surface charge of the gold nanoparticle opposed the approach of additional particles, which insured only single particle placement. This is an extremely impressive result considering that the diameter of the *gate* is almost 7 times larger than that of the particle it isolated and could have been even better if the lithographic definition of the *gates* were more accurate. It is entirely likely that a combination of the techniques of the gating mechanism¹⁴⁹ and transfer printing^{163, 164} can be combined for electrically directed assembly;¹⁶⁵ incorporated into a probe configuration, this may be useful for the 3D printing of individual nanoparticles.

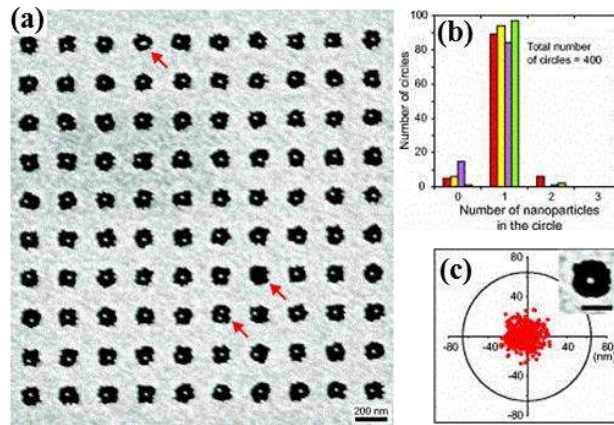


FIG. 18 Single nanoparticle capture in an array by self-assembly. SEM images of 20 nm Au particles self-assembled onto a surface patterned with gates. (b) Histogram of the number of nanoparticles captured on each of 400 tested gates. (c) Superimposed plot for the positions of single nanoparticles. Inset: SEM image of a gate containing one Au nanoparticle. Reproduced from¹⁴⁹.

In conclusion, single particle placement is able to build structures ranging from individual atoms up to hundreds of nanometres, but so far the throughput is very low and only useful for basic research and proof of concept designs. However, once commercially viable technologies have been discovered, increased automation will be able to increase the throughput. The possibility to combine self-assembly with one or more of the technologies described in this review is especially promising.

4. Discussion

It is clear that although additive nanomanufacturing may not be suited to replace CMOS (Complementary metal–oxide–semiconductor), it is likely that emerging processes can provide rapid prototyping capabilities as well as the ability to manufacture one-off parts and products. ANM has the potential to enable the manufacturing of specialized components at the nanoscale. This draws a close parallel with macro-scale additive manufacturing that started off as an expensive tool to now being present in many school classrooms. Several ANM methods have been reviewed in this article, and we summarize the key capabilities of these in this section.

ANM covers a large spectrum of technologies each with their strengths and weaknesses. The criteria for successful ANM are: design flexibility in the choice of materials and shape, resolution, writing speed/cost per unit, and initial investment cost. It is in the context of these criteria that future additive manufacturing techniques will be evaluated. As with all novel emerging technologies, it is worthwhile remembering that no

one technology can provide the solution for all future manufacturing needs. However, in combination most of these needs can be met.

Single particle placement technologies such as STM, AFM manipulation, and optical tweezers are comparatively slow but they may be able to enable quantum computing¹²⁰ or advance fundamental research through proof-of-principle device fabrication. Self-assembly is essentially how nature works and in the future it is likely that bio-inspired self-assembly in combination with ANM will create novel structures on a large scale. So far self-assembly is in its infancy but as a tool to control wettability⁷³ and adhesion¹⁶ or guide charged particles¹⁴⁹ self-assembled monolayers (SAMs) have found extensive use.¹⁶⁶

Method	Materials	Speed	Min. Feature Size	References
STM	Single atoms (e.g. Xe)	< 1 nm/s*	atomic	114, 118, 130
AFM manipulation	Single atoms (e.g. Sn), any nanoscale object (e.g. carbon nanotubes, nanoparticles)	< 10 nm/s*	atomic	116, 125, 129, 167
Dip-pen Nanolithography (DPN)	From small organic molecules to organic and biological polymers and from colloidal particles to metal ions and sols	Increased with the number of probes: DPL < 2D arrays < PPL	15 nm resolution on single crystal surfaces, <50 nm on polycrystalline surfaces	23, 36, 168, 169, 170
EHD Jet Printing	Metal nanoparticles, polymers, block copolymers	80 mm/s	10 nm	73, 74, 79, 86
Direct Laser Writing (DLW)	Polymers, metals	100 μm/s	65 nm, 22 nm	96, 101

Table I List of the materials, deposition speed, and minimum feature size reported for each additive nanomanufacturing technology.

*=Estimated.

Dip-pen lithography (DPN) has been shown to offer an excellent selection of both organic and inorganic materials with sub-50 nm resolution. In the course of the development of this technology, the traditional cantilever structure has been replaced by cantilever-free systems and arrays of probes. So far, the resolution is limited by the size of both the tip and the meniscus forming between the tip and the substrate. For many biological applications the current resolution is adequate; in fact, DPN is a powerful research tool for manipulating cells at subcellular resolution¹⁷¹ and changing the growth conditions for these cells. This resolution is, however, not sufficient for the future of Integrated Circuit (IC) manufacturing, but closely related lithography methods such as local anodic oxidation reach sub-10 nm resolution¹⁷² proving that better

resolution is possible with DPN when combined with an electrically driven reaction. DPN has so far been a two-dimensional lithography technique but the technology is very flexible with an inbuilt imaging capability and extending it into the third dimension seems plausible in the near future.

Electrohydrodynamic (EHD) jet printing has gone through a rapid development in the last couple of years with resolutions now reaching sub-50 nm^{73, 79} or sub-10 nm when combined with block copolymer technologies.⁷⁴ The writing speed is unparalleled when compared to other additive manufacturing technologies presented here (see Table I) and is comparable to the writing speed of EBL. Additionally EHD is capable of printing in three dimensions⁷³ and because the material is deposited through a solvent, a wide range of materials can be available. The equipment requirements are basic, so equipment cost can be kept low. The main challenges are nozzle clogging and layer-to-layer alignment but these are not insurmountable problems making EHD a promising candidate for future ANM.

Direct laser writing (DLW) offers great flexibility and was one of the first technologies capable of three-dimensional manufacturing at the nanoscale. It has proven invaluable for fabrication of three-dimensional photonic structures and has already had commercial success. Despite this success DLW has drawbacks particularly because material selection is still limited in spite of it being a relatively mature technology.

Direct write nanomanufacturing is still not able to produce the billions of structures needed for the IC industry, but neither is macro-scale additive manufacturing able to compete with the cost per unit of injection moulding and other mass-fabrication methods. Macro-scale additive manufacturing first found a home in niche areas of dental and medical care, aerospace, automotive and entertainment; nevertheless, macro-scale additive manufacturing is on the rise and the market is predicted to double from 2011 to 2015¹. ANM will have to start out with markets smaller than IC manufacturing and the smaller investment needed for ANM equipment will help this development.

Currently an IC manufacturing plant costs around \$9 billion; an ANM unit at <\$500,000 would be transformational for small and medium size firms to own their manufacturing facilities. Additionally, the way designers think will change as three-dimensional structures become readily available and the low material waste enables the use of expensive materials such as proteins in bio-sensors. There is also a potential environmental gain to using ANM over planar device fabrication as a traditionally built 2 g silicon chip requires

1.6 kg of fossil fuel, 73 g of chemicals and 32 kg of water.^{20, 173} Research into additive nanomanufacture could focus on cutting this environmental impact, for example by eliminating waste by directly placing materials where needed. Additionally, ideas that previously had no future because the market did not require the millions of sold units needed to break-even may now become viable. The unit price of direct writing does not depend on the density of the printed structures, as is the case for planar device fabrication, but rather depends on the total printed area. For a chemical or biomarker sensor the detector area might be much smaller than the minimum die size and planar manufacturing could become prohibitively expensive. The aspect of resolution as compared to semiconductor manufacturing is also seeing progress; the resolution of some of these techniques has reached a level where it can compete with that of EUV-lithography. They are well suited to a range of materials, not just “CMOS-Compatible” materials; Table I summarizes a subset of the available materials possible in each of these technologies.

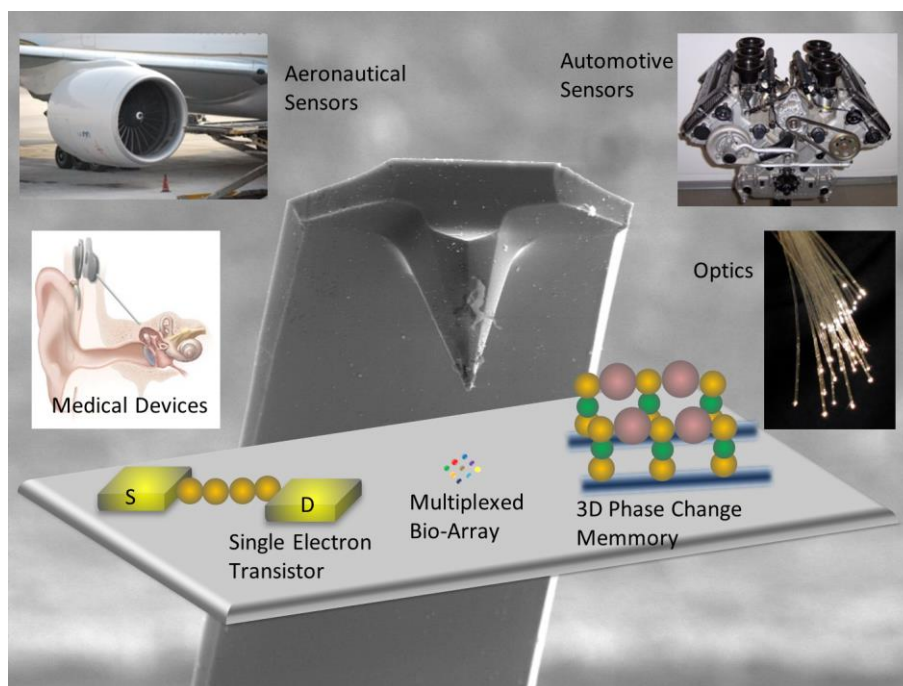


FIG. 19 Additive nanomanufacturing in the coming decade is likely to fabricate single electron transistors, multiplexed bio-arrays and 3D phase change memory. Devices and sensors could be directly printed on existing technologies within aeronautical, automotive, medical and optical industries.

The future of ANM relies on these technologies to either enable fabrication of structures that cannot otherwise be built or add functionality to existing technologies. One example where ANM can enable new structures is the assembly of nanoparticles into functional devices. It has been shown that a wire of gold

nanoparticles can be used as single electron transistors¹⁷⁴ but it is currently almost impossible to mass-manufacture such structures. Probe-based pick-and-place ANM can accurately position nanoparticles in the desired configuration making such devices possible in the future (See FIG. 19). Phase change memory devices are another example where ANM might enable a new technology. The device is a three-dimensional structure which is inherently difficult to fabricate using planar technologies and the ability to build these structures from individual nanocomponents using ANM is a real possibility. Promising biological applications of macro-scale additive manufacturing are three-dimensional scaffolds for bone and tissue growth,^{175, 176} direct printing of cells for organ growth as well as creating biocompatible films for drug delivery.¹⁷⁷ At the nanoscale ANM has the capability to fabricate structures from a sub-cellular level to sizes suitable for cellular scaffolds (cells are 1-100 μm in diameter). Biological applications of ANM include bio-arrays for screening, micro- and nanoscale robotics, bio-sensing, and biocompatible environments for cell growth. In biology multiplexing is of great importance due to the vast amount of proteins and small molecules found in living organisms. One of the challenges for bio-ANM will be to deposit single molecules; the ability to add parts of molecular functional elements, such as ion channels or molecular motors using ATP to harvest energy, will enable the study of individual cellular reactions or the creation of bionic micro-robots. Biocompatibility is an area of importance for bio-scaffolds and stem cells have especially proven difficult to grow *in-vitro*. The growth is affected by cell adhesion to the substrate, chemical growth, small-molecule extracellular signalling and mechanical strain.¹⁷⁸ ANM technologies such as EHD Jet printing have the ability to print protein fibres with sub-cellular resolution⁸⁴ which could solve some of the biocompatibility problems and potentially accelerate growth in the field. The challenge will be to build biocompatible or living structures in three-dimensions rapidly for medical applications. For electrochemical electrode array-based bio-sensing, smaller dimensions increase sensitivity via better signal-to-noise ratio, lower detection limits, and superior temporal resolution. Optimizing this electrode array design can improve diffusion of the reactive species to the electrode array or increase the surface area for increased sensitivity and it will be a challenge for ANM to show the flexibility to improve bio-sensing through design and material choice.

Direct writing of graphene might also be possible in the future by allowing an AFM tip coated with graphite to slide over a surface, thereby leaving a nanoribbon/monolayer of exfoliated graphene. This would be an

improvement of the results by Zhang et al¹⁷⁹ who used a mounted graphite block on the cantilever as the tip of an atomic force microscope in order to transfer thin graphite samples onto a SiO₂/Si substrate. "Writing" with the nanopencil yielded slices of graphite just a few tens of atomic layers thick, thereby almost succeeding in direct writing of graphene. This could enable device fabrication and repairing or modification of existing circuits to tailor functionality.

Other areas in which ANM can solve fabrication challenges in the future are photonic crystals, metamaterials such as negative refractive index materials and invisibility cloaks, electrochemical reactors, and high-density electronics.

Adding functionality to existing structures is also a way ANM can contribute in the future. For example, electronics could be printed directly at the end of an optical fibre thereby integrating optics and electronics in ways never seen before, and sensors can be printed directly onto engine parts or medical devices. ANM would also enable fully integrated devices including electronic, optical, and biochemical elements.

In conclusion, we have reviewed both single particle placement and direct writing technologies able to create sub-100 nm structures. We have especially focused on their ability to create heterogeneous structures from multiple materials and the possibility to extend fabrication into the third dimension. We identified single particle placement technologies such as STM, AFM manipulation, and optical tweezers as enablers of technological advances but not as future manufacturing tools. Direct writing technologies, on the other hand, offer a much more promising future of design flexibility, high resolution and high throughput. DLW offers high geometrical flexibility and medium throughput but currently suffers from a poor selection of materials. DPN is a reasonably mature technology with a wide material selection and promises of sub-10 nm resolution. The technology can be scaled up and currently the main challenges are to print in three dimensions and combine more functional materials. EHD Jet Printing is a simple and inexpensive technology that offers writing speeds comparable to e-beam lithography with high resolution (~20 nm) and great material choice. Additionally, three-dimensional structures of only 50 nm wide have been printed proving the possibility of true 3D additive nanomanufacturing.

Within the next few years we predict a rapid development of the ANM technologies presented here, especially towards 3D ANM. This new capability will inevitably lead to more innovation as new applications emerge. If

ANM follows the development trajectory of the last decade, its rise as a nanoscale rapid prototyping tool will soon be imminent.

References

1. F. Feenstra, M. Schaefer, O. Jay, and R. Scudamore: Additive Manufacturing: Strategic Research Agenda. *AM Platform: The European collaboration on Additive Manufacturing* **1** (1), 1 (2013).
2. T. Boland, A. Ovsianikov, B. N. Chickov, A. Doraiswamy, R. J. Narayan, W. Y. Yeong, K. F. Leong, and C. K. Chua: Rapid prototyping of artificial tissues and medical devices. *Adv Mater Process* **165** (4), 51 (2007).
3. I. Zein, D. W. Hutmacher, K. C. Tan, and S. H. Teoh: Fused deposition modeling of novel scaffold architectures for tissue engineering applications. *Biomaterials* **23** (4), 1169 (2002).
4. A. C. Arias, J. D. MacKenzie, I. McCulloch, J. Rivnay, and A. Salleo: Materials and Applications for Large Area Electronics: Solution-Based Approaches. *Chem Rev* **110** (1), 3 (2010).
5. L. L. Zhang, X. Zhao, M. D. Stoller, Y. W. Zhu, H. X. Ji, S. Murali, Y. P. Wu, S. Peralas, B. Clevenger, and R. S. Ruoff: Highly Conductive and Porous Activated Reduced Graphene Oxide Films for High-Power Supercapacitors. *Nano letters* **12** (4), 1806 (2012).
6. D. C. Duffy, J. C. McDonald, O. J. A. Schueller, and G. M. Whitesides: Rapid prototyping of microfluidic systems in poly(dimethylsiloxane). *Anal Chem* **70** (23), 4974 (1998).
7. M. A. Unger, H. P. Chou, T. Thorsen, A. Scherer, and S. R. Quake: Monolithic microfabricated valves and pumps by multilayer soft lithography. *Science* **288** (5463), 113 (2000).
8. R. van Noort: The future of dental devices is digital. *Dent Mater* **28** (1), 3 (2012).
9. G. Ryan, A. Pandit, and D. P. Apatsidis: Fabrication methods of porous metals for use in orthopaedic applications. *Biomaterials* **27** (13), 2651 (2006).
10. J. Giannatsis, and V. Dedoussis: Additive fabrication technologies applied to medicine and health care: a review. *Int J Adv Manuf Tech* **40** (1-2), 116 (2009).
11. R. J. Narayan, A. Doraiswamy, D. B. Chrisey, and B. N. Chichkov: Medical prototyping using two photon polymerization. *Mater Today* **13** (12), 42 (2010).
12. D. D. Gu, W. Meiners, K. Wissenbach, and R. Poprawe: Laser additive manufacturing of metallic components: materials, processes and mechanisms. *Int Mater Rev* **57** (3), 133 (2012).
13. Y. Jang, I. H. Tambunan, H. Tak, V. D. Nguyen, T. Kang, and D. Byun: Non-contact printing of high aspect ratio Ag electrodes for polycrystalline silicon solar cell with electrohydrodynamic jet printing. *Applied Physics Letters* **102** (12), (2013).
14. F. C. Krebs: Fabrication and processing of polymer solar cells: A review of printing and coating techniques. *Sol Energ Mat Sol C* **93** (4), 394 (2009).
15. A. G. Mark, J. G. Gibbs, T. C. Lee, and P. Fischer: Hybrid nanocolloids with programmed three-dimensional shape and material composition. *Nat Mater* **12** (9), 802 (2013).
16. J. U. Park, M. Hardy, S. J. Kang, K. Barton, K. Adair, D. K. Mukhopadhyay, C. Y. Lee, M. S. Strano, A. G. Alleyne, J. G. Georgiadis, P. M. Ferreira, and J. A. Rogers: High-resolution electrohydrodynamic jet printing. *Nat Mater* **6** (10), 782 (2007).
17. S. Y. Min, T. S. Kim, B. J. Kim, H. Cho, Y. Y. Noh, H. Yang, J. H. Cho, and T. W. Lee: Large-scale organic nanowire lithography and electronics. *Nat Commun* **4**, 1773 (2013).
18. C. Wagner, and N. Harned: EUV LITHOGRAPHY Lithography gets extreme. *Nat Photonics* **4** (1), 24 (2010).
19. V. R. Manfrinato, L. H. Zhang, D. Su, H. G. Duan, R. G. Hobbs, E. A. Stach, and K. K. Berggren: Resolution Limits of Electron-Beam Lithography toward the Atomic Scale. *Nano letters* **13** (4), 1555 (2013).
20. E. D. Williams, R. U. Ayres, and M. Heller: The 1.7 kilogram microchip: Energy and material use in the production of semiconductor devices. *Environ Sci Technol* **36** (24), 5504 (2002).
21. P. R. Couchman, and W. A. Jesser: Thermodynamic Theory of Size Dependence of Melting Temperature in Metals. *Nature* **269** (5628), 481 (1977).
22. G. L. Allen, R. A. Bayles, W. W. Gile, and W. A. Jesser: Small Particle Melting of Pure Metals. *Thin Solid Films* **144** (2), 297 (1986).
23. D. S. Ginger, H. Zhang, and C. A. Mirkin: The Evolution of Dip-Pen Nanolithography. *Angewandte Chemie International Edition* **43** (1), 30 (2004).
24. G. Binnig, H. Rohrer, C. Gerber, and E. Weibel: Surface Studies by Scanning Tunneling Microscopy. *Physical Review Letters* **49** (1), 57 (1982).

25. G. Binnig, C. F. Quate, and C. Gerber: Atomic Force Microscope. *Physical Review Letters* **56** (9), 930 (1986).
26. J. K. Gimzewski, and C. Joachim: Nanoscale Science of Single Molecules Using Local Probes. *Science* **283** (5408), 1683 (1999).
27. D. M. S. Eigler, E. K.: Positioning single atoms with a scanning tunnelling microscope. *Nature* **344** (6266), 524 (1990).
28. Y. Xia, and G. M. Whitesides: Soft Lithography. *Angewandte Chemie International Edition* **37** (5), 550 (1998).
29. J.-F. Liu, S. Cruchon-Dupeyrat, J. C. Garno, J. Frommer, and G.-Y. Liu: Three-Dimensional Nanostructure Construction via Nanografting: Positive and Negative Pattern Transfer. *Nano Letters* **2** (9), 937 (2002).
30. S. C. Minne, S. R. Manalis, A. Atalar, and C. F. Quate: Independent parallel lithography using the atomic force microscope. *Journal of Vacuum Science & Technology B* **14** (4), 2456 (1996).
31. S. C. Minne, J. D. Adams, G. Yaralioglu, S. R. Manalis, A. Atalar, and C. F. Quate: Centimeter scale atomic force microscope imaging and lithography. *Applied Physics Letters* **73** (12), 1742 (1998).
32. K. W. Salaita, Yuhuang Mirkin, Chad A.: Applications of dip-pen nanolithography. *Nat Nano* **2** (3), (2007).
33. K. Brown, D. Eichelsdoerfer, X. Liao, S. He, and C. Mirkin: Material transport in dip-pen nanolithography. *Frontiers of Physics*, 1 (2013).
34. B. D. Gates, Q. Xu, M. Stewart, D. Ryan, C. G. Willson, and G. M. Whitesides: New Approaches to Nanofabrication: Molding, Printing, and Other Techniques. *Chemical Reviews* **105** (4), 1171 (2005).
35. H. Zhang, and C. A. Mirkin: DPN-Generated Nanostructures Made of Gold, Silver, and Palladium. *Chemistry of Materials* **16** (8), 1480 (2004).
36. R. D. Piner, J. Zhu, F. Xu, S. Hong, and C. A. Mirkin: "Dip-Pen" Nanolithography. *Science* **283** (5402), 661 (1999).
37. K. W. Salaita, Yuhuang Mirkin, Chad A.: Applications of dip-pen nanolithography. *Nat Nano* **2** (3), 145 (2007).
38. D. Nyamjav, and A. Ivanisevic: Properties of Polyelectrolyte Templates Generated by Dip-Pen Nanolithography and Microcontact Printing. *Chemistry of Materials* **16** (25), 5216 (2004).
39. R. Suriano, S. Biella, F. Cesura, M. Levi, and S. Turri: Thermoplastic polymers surfaces for Dip-Pen Nanolithography of oligonucleotides. *Applied Surface Science* **273** (0), 717 (2013).
40. S. Park, H. W. Lee, H. Wang, S. Selvarasah, M. R. Dokmeci, Y. J. Park, S. N. Cha, J. M. Kim, and Z. Bao: Highly Effective Separation of Semiconducting Carbon Nanotubes verified via Short-Channel Devices Fabricated Using Dip-Pen Nanolithography. *ACS Nano* **6** (3), 2487 (2012).
41. Y. Wang, D. Maspoch, S. Zou, G. C. Schatz, R. E. Smalley, and C. A. Mirkin: Controlling the shape, orientation, and linkage of carbon nanotube features with nano affinity templates. *Proceedings of the National Academy of Sciences of the United States of America* **103** (7), 2026 (2006).
42. Y. Li, B. W. Maynor, and J. Liu: Electrochemical AFM "dip-pen" nanolithography. *J Am Chem Soc* **123** (9), 2105 (2001).
43. L. Fu, X. Liu, Y. Zhang, V. P. Dravid, and C. A. Mirkin: Nanopatterning of "Hard" Magnetic Nanostructures via Dip-Pen Nanolithography and a Sol-Based Ink. *Nano Letters* **3** (6), 757 (2003).
44. S. Lenhart, P. Sun, Y. Wang, H. Fuchs, and C. A. Mirkin: Massively Parallel Dip-Pen Nanolithography of Heterogeneous Supported Phospholipid Multilayer Patterns. *Small* **3** (1), 71 (2007).
45. M. O. Hirtz, Antonios Georgiou, Thanasis Fuchs, Harald Vijayaraghavan, Aravind: Multiplexed biomimetic lipid membranes on graphene by dip-pen nanolithography. *Nat Commun* **4**, (2013).
46. K.-B. Lee, S.-J. Park, C. A. Mirkin, J. C. Smith, and M. Mrksich: Protein Nanoarrays Generated By Dip-Pen Nanolithography. *Science* **295** (5560), 1702 (2002).
47. K.-B. Lee, J.-H. Lim, and C. A. Mirkin: Protein Nanostructures Formed via Direct-Write Dip-Pen Nanolithography. *Journal of the American Chemical Society* **125** (19), 5588 (2003).
48. L. M. Demers, D. S. Ginger, S.-J. Park, Z. Li, S.-W. Chung, and C. A. Mirkin: Direct Patterning of Modified Oligonucleotides on Metals and Insulators by Dip-Pen Nanolithography. *Science* **296** (5574), 1836 (2002).
49. R. A. Vega, C. K. F. Shen, D. Maspoch, J. G. Robach, R. A. Lamb, and C. A. Mirkin: Monitoring Single-Cell Infectivity from Virus-Particle Nanoarrays Fabricated by Parallel Dip-Pen Nanolithography. *Small* **3** (9), 1482 (2007).

50. S. D. Cronin, K. Sabolsky, E. M. Sabolsky, and K. A. Sierros: Dip pen nanolithography and transfer of ZnO patterns on plastics for large-area flexible optoelectronic applications. *Thin Solid Films* **552** (0), 50 (2014).
51. K. Salaita, Y. Wang, J. Fragala, R. A. Vega, C. Liu, and C. A. Mirkin: Massively Parallel Dip-Pen Nanolithography with 55 000-Pen Two-Dimensional Arrays. *Angewandte Chemie International Edition* **45** (43), 7220 (2006).
52. W. Shim, A. B. Braunschweig, X. Liao, J. N. Chai, J. K. Lim, G. F. Zheng, and C. A. Mirkin: Hard-tip, soft-spring lithography. *Nature* **469** (7331), 516 (2011).
53. L. R. Giam, and C. A. Mirkin: Cantilever-Free Scanning Probe Molecular Printing. *Angewandte Chemie International Edition* **50** (33), 7482 (2011).
54. F. Huo, Z. Zheng, G. Zheng, L. R. Giam, H. Zhang, and C. A. Mirkin: Polymer Pen Lithography. *Science* **321** (5896), 1658 (2008).
55. J. Chai, F. Huo, Z. Zheng, L. R. Giam, W. Shim, and C. A. Mirkin: Scanning probe block copolymer lithography. *Proceedings of the National Academy of Sciences* **107** (47), 20202 (2010).
56. G. Liu, D. J. Eichelsdoerfer, B. Rasin, Y. Zhou, K. A. Brown, X. Liao, and C. A. Mirkin: Delineating the pathways for the site-directed synthesis of individual nanoparticles on surfaces. *Proceedings of the National Academy of Sciences* **110** (3), 887 (2013).
57. J. Chai, L. S. Wong, L. Giam, and C. A. Mirkin: Single-molecule protein arrays enabled by scanning probe block copolymer lithography. *Proceedings of the National Academy of Sciences* **108** (49), 19521 (2011).
58. K. A. Brown, D. J. Eichelsdoerfer, W. Shim, B. Rasin, B. Radha, X. Liao, A. L. Schmucker, G. Liu, and C. A. Mirkin: A cantilever-free approach to dot-matrix nanoprinting. *Proceedings of the National Academy of Sciences* **110** (32), 12921 (2013).
59. S. D. Bian, S. B. Zieba, W. Morris, X. Han, D. C. Richter, K. A. Brown, C. A. Mirkin, and A. B. Braunschweig: Beam pen lithography as a new tool for spatially controlled photochemistry, and its utilization in the synthesis of multivalent glycan arrays. *Chem Sci* **5** (5), 2023 (2014).
60. J. M. Curran, R. Chen, R. Stokes, E. Irvine, D. Graham, E. Gubbins, D. Delaney, N. Amro, R. Sanedrin, H. Jamil, and J. A. Hunt: Nanoscale definition of substrate materials to direct human adult stem cells towards tissue specific populations. *J Mater Sci-Mater M* **21** (3), 1021 (2010).
61. S. Sekula, J. Fuchs, S. Weg-Remers, P. Nagel, S. Schuppler, J. Fragala, N. Theilacker, M. Franueb, C. Wingren, P. Ellmark, C. A. K. Borrebaeck, C. A. Mirkin, H. Fuchs, and S. Lenhert: Multiplexed Lipid Dip-Pen Nanolithography on Subcellular Scales for the Templating of Functional Proteins and Cell Culture. *Small* **4** (10), 1785 (2008).
62. K. Mitsakakis, S. Sekula-Neuner, S. Lenhert, H. Fuchs, and E. Gizeli: Convergence of Dip-Pen Nanolithography and acoustic biosensors towards a rapid-analysis multi-sample microsystem. *Analyst* **137** (13), 3076 (2012).
63. X. Z. Zhou, F. Boey, F. W. Huo, L. Huang, and H. Zhang: Chemically Functionalized Surface Patterning. *Small* **7** (16), 2273 (2011).
64. C. C. Wu, D. N. Reinhoudt, C. Otto, V. Subramaniam, and A. H. Velders: Strategies for Patterning Biomolecules with Dip-Pen Nanolithography. *Small* **7** (8), 989 (2011).
65. H. Bhaskaran, B. Gotsmann, A. Sebastian, U. Drechsler, M. A. Lantz, M. Despont, P. Jaroenapibal, R. W. Carpick, Y. Chen, and K. Sridharan: Ultralow nanoscale wear through atom-by-atom attrition in silicon-containing diamond-like carbon. *Nat Nanotechnol* **5** (3), 181 (2010).
66. H. Bhaskaran, A. Sebastian, and M. Despont: Nanoscale PtSi Tips for Conducting Probe Technologies. *Ieee T Nanotechnol* **8** (1), 128 (2009).
67. H. Bhaskaran, A. Sebastian, U. Drechsler, and M. Despont: Encapsulated tips for reliable nanoscale conduction in scanning probe technologies. *Nanotechnology* **20** (10), (2009).
68. P. C. Fletcher, J. R. Felts, Z. T. Dai, T. D. Jacobs, H. J. Zeng, W. Lee, P. E. Sheehan, J. A. Carlisle, R. W. Carpick, and W. P. King: Wear-Resistant Diamond Nanoprobe Tips with Integrated Silicon Heater for Tip-Based Nanomanufacturing. *Acs Nano* **4** (6), 3338 (2010).
69. J. T. Delaney, P. J. Smith, and U. S. Schubert: Inkjet printing of proteins. *Soft Matter* **5** (24), 4866 (2009).
70. S. B. Fuller, E. J. Wilhelm, and J. M. Jacobson: Ink-jet printed nanoparticle microelectromechanical systems. *J Microelectromech S* **11** (1), 54 (2002).

71. H. K. Choi, J. U. Park, O. O. Park, P. M. Ferreira, J. G. Georgiadis, and J. A. Rogers: Scaling laws for jet pulsations associated with high-resolution electrohydrodynamic printing. *Applied Physics Letters* **92** (12), (2008).
72. A. Barrero, and I. G. Loscertales: Micro- and nanoparticles via capillary flows. *Annu Rev Fluid Mech* **39**, 89 (2007).
73. P. Galliker, J. Schneider, H. Eghlidi, S. Kress, V. Sandoghdar, and D. Poulikakos: Direct printing of nanostructures by electrostatic autofocussing of ink nanodroplets. *Nat Commun* **3**, (2012).
74. M. S. Onses, C. Song, L. Williamson, E. Sutanto, P. M. Ferreira, A. G. Alleyne, P. F. Nealey, H. Ahn, and J. A. Rogers: Hierarchical patterns of three-dimensional block-copolymer films formed by electrohydrodynamic jet printing and self-assembly. *Nat Nanotechnol* **8** (9), 667 (2013).
75. M. Lee, and H. Y. Kim: Toward Nanoscale Three-Dimensional Printing: Nanowalls Built of Electrospun Nanofibers. *Langmuir : the ACS journal of surfaces and colloids* **30** (5), 1210 (2014).
76. Y. Huang, N. Bu, Y. Duan, Y. Pan, H. Liu, Z. Yin, and Y. Xiong: Electrohydrodynamic direct-writing. *Nanoscale* **5** (24), 12007 (2013).
77. B. Sundaray, V. Subramanian, T. S. Natarajan, R. Z. Xiang, C. C. Chang, and W. S. Fann: Electrospinning of continuous aligned polymer fibers. *Applied Physics Letters* **84** (7), 1222 (2004).
78. Y. A. Huang, X. M. Wang, Y. Q. Duan, N. B. Bu, and Z. P. Yin: Controllable self-organization of colloid microarrays based on finite length effects of electrospun ribbons. *Soft Matter* **8** (32), 8302 (2012).
79. G. S. Bisht, G. Canton, A. Mirsepassi, L. Kuinsky, S. Oh, D. Dunn-Rankin, and M. J. Madou: Controlled Continuous Patterning of Polymeric Nanofibers on Three-Dimensional Substrates Using Low-Voltage Near-Field Electrospinning. *Nano letters* **11** (4), 1831 (2011).
80. N. Bu, Y. Huang, X. Wang, and Z. Yin: Continuously Tunable and Oriented Nanofiber Direct-Written by Mechano-Electrospinning. *Mater. Manuf. Processes* **27** (12), 1318 (2012).
81. D. Li, and Y. N. Xia: Direct fabrication of composite and ceramic hollow nanofibers by electrospinning. *Nano letters* **4** (5), 933 (2004).
82. Y. Z. Zhang, X. Wang, Y. Feng, J. Li, C. T. Lim, and S. Ramakrishna: Coaxial electrospinning of (fluorescein isothiocyanate-conjugated bovine serum albumin)-encapsulated poly(epsilon-caprolactone) nanofibers for sustained release. *Biomacromolecules* **7** (4), 1049 (2006).
83. D. Z. Wang, S. N. Jayasinghe, M. J. Edirisinghe, and Z. B. Luklinska: Coaxial electrohydrodynamic direct writing of nano-suspensions. *J Nanopart Res* **9** (5), 825 (2007).
84. W. Nuansing, D. Frauchiger, F. Huth, A. Rebollo, R. Hillenbrand, and A. M. Bittner: Electrospinning of peptide and protein fibres: approaching the molecular scale. *Faraday Discuss* **166**, 209 (2013).
85. O. V. Salata: Tools of nanotechnology: Electropray. *Curr Nanosci* **1** (1), 25 (2005).
86. A. Jaworek, and A. T. Sobczyk: Electro spraying route to nanotechnology: An overview. *J Electrostat* **66** (3-4), 197 (2008).
87. D. Y. Lee, Y. S. Shin, S. E. Park, T. U. Yu, and J. Hwang: Electrohydrodynamic printing of silver nanoparticles by using a focused nanocolloid jet. *Applied Physics Letters* **90** (8), (2007).
88. S. Kawata, H. B. Sun, T. Tanaka, and K. Takada: Finer features for functional microdevices. *Nature* **412** (6848), 697 (2001).
89. M. Deubel, G. von Freymann, M. Wegener, S. Pereira, K. Busch, and C. M. Soukoulis: Direct laser writing of three-dimensional photonic-crystal templates for telecommunications. *Nature materials* **3** (7), 444 (2004).
90. T. Ergin, N. Stenger, P. Brenner, J. B. Pendry, and M. Wegener: Three-dimensional invisibility cloak at optical wavelengths. *Science (New York, N.Y.)* **328** (5976), 337 (2010).
91. J. Fischer, T. Ergin, and M. Wegener: Three-dimensional polarization-independent visible-frequency carpet invisibility cloak. *Optics Letters* **36** (11), 2059 (2011).
92. M. Röhrig, M. Thiel, M. Worgull, and H. Hölscher: 3D direct laser writing of nano- and microstructured hierarchical gecko-mimicking surfaces. *Small (Weinheim an der Bergstrasse, Germany)* **8** (19), 3009 (2012).
93. X. Li, Y. Cao, and M. Gu: Superresolution-focal-volume induced 3.0 Tbytes/disk capacity by focusing a radially polarized beam. *Optics letters* **36** (13), 2510 (2011).
94. B.-B. Xu, H. Xia, L.-G. Niu, Y.-L. Zhang, K. Sun, Q.-D. Chen, Y. Xu, Z.-Q. Lv, Z.-H. Li, H. Misawa, and H.-B. Sun: Flexible nanowiring of metal on nonplanar substrates by femtosecond-laser-induced electroless plating. *Small (Weinheim an der Bergstrasse, Germany)* **6** (16), 1762 (2010).

95. J. Fischer, and M. Wegener: Three-dimensional direct laser writing inspired by stimulated-emission-depletion microscopy. *Optical Materials Express* **1** (4), 614 (2011).
96. Y. Cao, and M. Gu: $\Lambda/26$ Silver Nanodots Fabricated By Direct Laser Writing Through Highly Sensitive Two-Photon Photoreduction. *Applied Physics Letters* **103** (21), 213104 (2013).
97. E. Kabouraki, A. N. Giakoumaki, P. Danilevicius, D. Gray, M. Vamvakaki, and M. Farsari: Redox multiphoton polymerization for 3D nanofabrication. *Nano letters* **13** (8), 3831 (2013).
98. N. Vasilantonakis, K. Terzaki, I. Sakellari, V. Purlys, D. Gray, C. M. Soukoulis, M. Vamvakaki, M. Kafesaki, and M. Farsari: Three-dimensional metallic photonic crystals with optical bandgaps. *Advanced materials (Deerfield Beach, Fla.)* **24** (8), 1101 (2012).
99. I. Staude, M. Decker, M. J. Ventura, C. Jagadish, D. N. Neshev, M. Gu, and Y. S. Kivshar: Hybrid high-resolution three-dimensional nanofabrication for metamaterials and nanoplasmonics. *Advanced materials (Deerfield Beach, Fla.)* **25** (9), 1260 (2013).
100. A. Frölich, J. Fischer, T. Zebrowski, K. Busch, and M. Wegener: Titania woodpiles with complete three-dimensional photonic bandgaps in the visible. *Advanced materials (Deerfield Beach, Fla.)* **25** (26), 3588 (2013).
101. J. Fischer, and M. Wegener: Three-dimensional optical laser lithography beyond the diffraction limit. *Laser & Photonics Reviews* **7** (1), 22 (2013).
102. Y. Cao, Z. Gan, B. Jia, R. a. Evans, and M. Gu: High-photosensitive resin for super-resolution direct-laser-writing based on photoinhibited polymerization. *Optics express* **19** (20), 19486 (2011).
103. E. Rittweger, K. Y. Han, S. E. Irvine, C. Eggeling, and S. W. Hell: STED microscopy reveals crystal colour centres with nanometric resolution. *Nature Photonics* **3** (March), 1 (2009).
104. J. Fischer, G. von Freymann, and M. Wegener: The materials challenge in diffraction-unlimited direct-laser-writing optical lithography. *Advanced materials (Deerfield Beach, Fla.)* **22** (32), 3578 (2010).
105. M. F. El-Kady, and R. B. Kaner: Scalable fabrication of high-power graphene micro-supercapacitors for flexible and on-chip energy storage. *Nature communications* **4**, 1475 (2013).
106. J. B. Park, W. Xiong, Y. Gao, M. Qian, Z. Q. Xie, M. Mitchell, Y. S. Zhou, G. H. Han, L. Jiang, and Y. F. Lu: Fast growth of graphene patterns by laser direct writing. *Applied Physics Letters* **98** (12), 123109 (2011).
107. K. Kwok, and W. K. S. Chiu: Growth of carbon nanotubes by open-air laser-induced chemical vapor deposition. *Carbon* **43** (2), 437 (2005).
108. M. Mahjouri-Samani, Y. S. Zhou, W. Xiong, Y. Gao, M. Mitchell, L. Jiang, and Y. F. Lu: Diameter modulation by fast temperature control in laser-assisted chemical vapor deposition of single-walled carbon nanotubes. *Nanotechnology* **21** (39), 395601 (2010).
109. S. Hong, J. Yeo, G. Kim, D. Kim, H. H. Lee, J. Kwon, P. Lee, and S. H. Ko: Nonvacuum, maskless fabrication of a flexible metal grid transparent conductor by low-temperature selective laser sintering of nanoparticle ink. *ACS nano* **7** (6), 5024 (2013).
110. X. Liao, K. A. Brown, A. L. Schmucker, G. L. Liu, S. He, W. Shim, and C. A. Mirkin: Desktop nanofabrication with massively multiplexed beam pen lithography. *Nat Commun* **4**, (2013).
111. G. J. Leggett: Scanning near-field photolithography-surface photochemistry with nanoscale spatial resolution. *Chem Soc Rev* **35** (11), 1150 (2006).
112. E. ul Haq, Z. M. Liu, Y. A. Zhang, S. A. A. Ahmad, L. S. Wong, S. P. Armes, J. K. Hobbs, G. J. Leggett, J. Micklefield, C. J. Roberts, and J. M. R. Weaver: Parallel Scanning Near-Field Photolithography: The Snomipede. *Nano letters* **10** (11), 4375 (2010).
113. W. Srituravanich, L. Pan, Y. Wang, C. Sun, D. B. Bogy, and X. Zhang: Flying plasmonic lens in the near field for high-speed nanolithography. *Nat Nanotechnol* **3** (12), 733 (2008).
114. D. M. Eigler, and E. K. Schweizer: Positioning Single Atoms with a Scanning Tunneling Microscope. *Nature* **344** (6266), 524 (1990).
115. Y. Sugimoto, M. Abe, S. Hirayama, N. Oyabu, O. Custance, and S. Morita: Atom inlays performed at room temperature using atomic force microscopy. *Nat Mater* **4** (2), 156 (2005).
116. O. Custance, R. Perez, and S. Morita: Atomic force microscopy as a tool for atom manipulation. *Nat Nanotechnol* **4** (12), 803 (2009).
117. D. Gohlke, R. Mishra, O. D. Restrepo, D. Lee, W. Windl, and J. Gupta: Atomic-Scale Engineering of the Electrostatic Landscape of Semiconductor Surfaces. *Nano letters* **13** (6), 2418 (2013).

118. D. A. Olyanich, V. G. Kotlyar, T. V. Utas, A. V. Zotov, and A. A. Saranin: The manipulation of C-60 in molecular arrays with an STM tip in regimes below the decomposition threshold. *Nanotechnology* **24** (5), (2013).
119. K. Morgenstern, N. Lorente, and K. H. Rieder: Controlled manipulation of single atoms and small molecules using the scanning tunnelling microscope. *Phys Status Solidi B* **250** (9), 1671 (2013).
120. M. Fuechsle, J. A. Miwa, S. Mahapatra, H. Ryu, S. Lee, O. Warschkow, L. C. L. Hollenberg, G. Klimeck, and M. Y. Simmons: A single-atom transistor. *Nat Nanotechnol* **7** (4), 242 (2012).
121. S. Y. Qin, T. H. Kim, Z. H. Wang, and A. P. Li: Nanomanipulation and nanofabrication with multi-probe scanning tunneling microscope: From individual atoms to nanowires. *Rev Sci Instrum* **83** (6), (2012).
122. K. Molhave, T. Wich, A. Kortschack, and P. Boggild: Pick-and-place nanomanipulation using microfabricated grippers. *Nanotechnology* **17** (10), 2434 (2006).
123. O. Sardan, V. Eichhorn, D. H. Petersen, S. Fatikow, O. Sigmund, and P. Boggild: Rapid prototyping of nanotube-based devices using topology-optimized microgrippers. *Nanotechnology* **19** (49), 495503 (2008).
124. A. Cagliani, R. Wierzbicki, L. Occhipinti, D. H. Petersen, K. N. Dyvelkov, O. S. Sukas, B. G. Herstrom, T. Booth, and P. Boggild: Manipulation and in situ transmission electron microscope characterization of sub-100 nm nanostructures using a microfabricated nanogripper. *J Micromech Microeng* **20** (3), (2010).
125. S. Kim, D. C. Ratchford, and X. Li: Atomic force microscope nanomanipulation with simultaneous visual guidance. *ACS nano* **3** (10), 2989 (2009).
126. S. Kim, F. Shafiei, D. Ratchford, and X. Li: Controlled AFM manipulation of small nanoparticles and assembly of hybrid nanostructures. *Nanotechnology* **22** (11), 115301 (2011).
127. J. Castillo, M. Dimaki, and W. E. Svendsen: Manipulation of biological samples using micro and nano techniques. *Integr Biol-Uk* **1** (1), 30 (2009).
128. T. Junno, K. Deppert, L. Montelius, and L. Samuelson: Controlled manipulation of nanoparticles with an atomic force microscope. *Applied Physics Letters* **66** (26), 3627 (1995).
129. J. Zhang, S. Member, N. Xi, and H. Chen: Design , Manufacturing , and Testing of Single-Carbon-Nanotube-Based Infrared Sensors. *IEEE Transactions on Nanotechnology* **8** (2), 245 (2009).
130. S. Qin, T.-H. Kim, Z. Wang, and A.-P. Li: Nanomanipulation and nanofabrication with multi-probe scanning tunneling microscope: from individual atoms to nanowires. *The Review of scientific instruments* **83** (6), 063704 (2012).
131. G. Li, N. Xi, M. Yu, and W.-K. Fung: Development of Augmented Reality System for AFM-Based Nanomanipulation. *IEEE Transactions on Nanotechnology* **9** (2), 358 (2004).
132. G. Li, N. Xi, H. Chen, C. Pomeroy, and M. Prokos: " Videolized " Atomic Force Microscopy for Interactive Nanomanipulation and Nanoassembly. *IEEE Transactions on Nanotechnology* **4** (5), 605 (2005).
133. N. Xi, and G. Li, *Introduction to Nanorobotic Manipulation and Assembly*. Artech House: Norwood, 2012; p 1.
134. X. Xiong, P. Makaram, A. Busnaina, K. Bakhtari, S. Somu, N. McGruer, and J. Park: Large scale directed assembly of nanoparticles using nanotrench templates. *Applied Physics Letters* **89** (19), 193108 (2006).
135. J.-U. Park, S. Lee, S. Unarunotai, Y. Sun, S. Dunham, T. Song, P. M. Ferreira, A. G. Alleyene, U. Paik, and J. a. Rogers: Nanoscale, electrified liquid jets for high-resolution printing of charge. *Nano letters* **10** (2), 584 (2010).
136. M. Kolíbal, M. Konečný, F. Ligmajer, D. Škoda, T. Vystavěl, J. Zlámal, P. Varga, and T. Šíkola: Guided assembly of gold colloidal nanoparticles on silicon substrates prepattered by charged particle beams. *ACS nano* **6** (11), 10098 (2012).
137. Y. S. Zhou, Y. Liu, G. Zhu, Z.-h. Lin, C. Pan, Q. Jing, and Z. L. Wang: In Situ Quantitative Study of Nanoscale Triboelectrification and Patterning. *Nano letters*, At press (2013).
138. A. G. Mark, J. G. Gibbs, T.-C. Lee, and P. Fischer: Hybrid nanocolloids with programmed three-dimensional shape and material composition. *Nature materials* **12** (9), 802 (2013).
139. C. Yilmaz, T.-H. Kim, S. Somu, and A. a. Busnaina: Large-Scale Nanorods Nanomanufacturing by Electric-Field-Directed Assembly for Nanoscale Device Applications. *IEEE Transactions on Nanotechnology* **9** (5), 653 (2010).
140. N. R. Wood, A. I. Wolsiefer, R. W. Cohn, and S. J. Williams: Dielectrophoretic trapping of nanoparticles with an electrokinetic nanoprobe. *Electrophoresis* **34** (13), 1922 (2013).

141. K. a. Brown, and R. M. Westervelt: Proposed triaxial atomic force microscope contact-free tweezers for nanoassembly. *Nanotechnology* **20** (38), 385302 (2009).
142. K. a. Brown, and R. M. Westervelt: Triaxial AFM probes for noncontact trapping and manipulation. *Nano Letters* **11** (8), 3197 (2011).
143. A. Jonás, and P. Zemánek: Light at work: the use of optical forces for particle manipulation, sorting, and analysis. *Electrophoresis* **29** (24), 4813 (2008).
144. L. Tong, V. D. Miljković, and M. Käll: Alignment, rotation, and spinning of single plasmonic nanoparticles and nanowires using polarization dependent optical forces. *Nano letters* **10** (1), 268 (2010).
145. M. J. Guffey, and N. F. Scherer: All-optical patterning of Au nanoparticles on surfaces using optical traps. *Nano letters* **10** (11), 4302 (2010).
146. Z. Yan, J. Sweet, J. E. Jureller, M. J. Guffey, M. Pelton, and N. F. Scherer: Controlling the position and orientation of single silver nanowires on a surface using structured optical fields. *ACS nano* **6** (9), 8144 (2012).
147. Z. Yan, R. a. Shah, G. Chado, S. K. Gray, M. Pelton, and N. F. Scherer: Guiding spatial arrangements of silver nanoparticles by optical binding interactions in shaped light fields. *ACS nano* **7** (2), 1790 (2013).
148. Y.-F. Chen, X. Serey, R. Sarkar, P. Chen, and D. Erickson: Controlled photonic manipulation of proteins and other nanomaterials. *Nano letters* **12** (3), 1633 (2012).
149. H.-W. Huang, P. Bhadrachalam, V. Ray, and S. J. Koh: Single-particle placement via self-limiting electrostatic gating. *Applied Physics Letters* **93** (7), 073110 (2008).
150. J. Berthelot, S. S. Aćimović, M. L. Juan, M. P. Kreuzer, J. Renger, and R. Quidant: Three-dimensional manipulation with scanning near-field optical nanotweezers. *Nat Nanotechnol*, (2014).
151. M. Fedoruk, M. Meixner, S. Carretero-Palacios, T. Lohmüller, and J. Feldmann: Nanolithography by Plasmonic Heating and Optical Manipulation of Gold Nanoparticles. *ACS nano*, At press (2013).
152. K. J. M. Bishop, C. E. Wilmer, S. Soh, and B. A. Grzybowski: Nanoscale Forces and Their Uses in Self-Assembly. *Small* **5** (14), 1600 (2009).
153. K. Sakakibara, J. P. Hill, and K. Ariga: Thin-film-based nanoarchitectures for soft matter: controlled assemblies into two-dimensional worlds. *Small (Weinheim an der Bergstrasse, Germany)* **7** (10), 1288 (2011).
154. S. J. Barrow, A. M. Funston, X. Z. Wei, and P. Mulvaney: DNA-directed self-assembly and optical properties of discrete 1D, 2D and 3D plasmonic structures. *Nano Today* **8** (2), 138 (2013).
155. J. X. Gong, G. D. Li, and Z. Y. Tang: Self-assembly of noble metal nanocrystals: Fabrication, optical property, and application. *Nano Today* **7** (6), 564 (2012).
156. E. Bellido, N. Domingo, I. Ojea-Jimenez, and D. Ruiz-Molina: Structuration and Integration of Magnetic Nanoparticles on Surfaces and Devices. *Small* **8** (10), 1465 (2012).
157. B. Dong, T. Zhou, H. Zhang, and C. Y. Li: Directed Self-Assembly of Nanoparticles for Nanomotors. *ACS nano*, At Press (2013).
158. J. F. Galisteo-López, M. Ibisate, R. Sapienza, L. S. Froufe-Pérez, A. Blanco, and C. López: Self-assembled photonic structures. *Advanced materials (Deerfield Beach, Fla.)* **23** (1), 30 (2011).
159. F. S. Kim, G. Ren, and S. a. Jenekhe: One-Dimensional Nanostructures of π -Conjugated Molecular Systems: Assembly, Properties, and Applications from Photovoltaics, Sensors, and Nanophotonics to Nanoelectronics †. *Chemistry of Materials* **23** (3), 682 (2011).
160. T. Kraus, L. Malaquin, H. Schmid, W. Riess, N. D. Spencer, and H. Wolf: Nanoparticle printing with single-particle resolution. *Nat Nanotechnol* **2** (9), 570 (2007).
161. H. Park, A. Afzali, S.-J. Han, G. S. Tulevski, A. D. Franklin, J. Tersoff, J. B. Hannon, and W. Haensch: High-density integration of carbon nanotubes via chemical self-assembly. *Nature nanotechnology* **7** (12), 787 (2012).
162. Y. Cui, M. T. Bjork, J. A. Liddle, C. Sonnichsen, B. Bousert, and A. P. Alivisatos: Integration of colloidal nanocrystals into lithographically patterned devices. *Nano letters* **4** (6), 1093 (2004).
163. A. Carlson, A. M. Bowen, Y. G. Huang, R. G. Nuzzo, and J. A. Rogers: Transfer Printing Techniques for Materials Assembly and Micro/Nanodevice Fabrication. *Advanced Materials* **24** (39), 5284 (2012).
164. Y. Zheng, C. H. Lalander, T. Thai, S. Dhuey, S. Cabrini, and U. Bach: Gutenberg-style printing of self-assembled nanoparticle arrays: electrostatic nanoparticle immobilization and DNA-mediated transfer. *Angewandte Chemie (International ed. in English)* **50** (19), 4398 (2011).

165. B. F. Porter, L. Abelmann, and H. Bhaskaran: Design parameters for voltage-controllable directed assembly of single nanoparticles. *Nanotechnology* **24** (40), 405304 (2013).
166. J. J. Gooding, and S. Ciampi: The molecular level modification of surfaces: from self-assembled monolayers to complex molecular assemblies. *Chem Soc Rev* **40** (5), 2704 (2011).
167. Y. Sugimoto, M. Abe, S. Hirayama, N. Oyabu, O. Custance, and S. Morita: Atom inlays performed at room temperature using atomic force microscopy. *Nature materials* **4** (2), 156 (2005).
168. S. Hong, and C. A. Mirkin: A Nanoplotter with Both Parallel and Serial Writing Capabilities. *Science* **288** (5472), 1808 (2000).
169. S. Hong, J. Zhu, and C. A. Mirkin: Multiple Ink Nanolithography: Toward a Multiple-Pen Nano-Plotter. *Science* **286** (5439), 523 (1999).
170. D. J. Pena, M. P. Raphael, and J. M. Byers: "Dip-Pen" Nanolithography in Registry with Photolithography for Biosensor Development. *Langmuir* **19** (21), 9028 (2003).
171. A. Pulsipher, and M. N. Yousaf: Surface Chemistry and Cell Biological Tools for the Analysis of Cell Adhesion and Migration. *ChemBioChem* **11** (6), 745 (2010).
172. J. Martinez, R. V. Martinez, and R. Garcia: Silicon Nanowire Transistors with a Channel Width of 4 nm Fabricated by Atomic Force Microscope Nanolithography. *Nano letters* **8** (11), 3636 (2008).
173. E. Williams: Energy intensity of computer manufacturing: Hybrid assessment combining process and economic input-output methods. *Environ Sci Technol* **38** (22), 6166 (2004).
174. J. Kane, M. Inan, and R. F. Saraf: Self-Assembled Nanoparticle Necklaces Network Showing Single-Electron Switching at Room Temperature and Biogating Current by Living Microorganisms. *Acs Nano* **4** (1), 317 (2010).
175. I. C. Bonzani, J. H. George, and M. M. Stevens: Novel materials for bone and cartilage regeneration. *Curr Opin Chem Biol* **10** (6), 568 (2006).
176. Q. P. Pham, U. Sharma, and A. G. Mikos: Electrospinning of polymeric nanofibers for tissue engineering applications: A review. *Tissue Eng* **12** (5), 1197 (2006).
177. B. C. Wang, Y. Z. Wang, T. Y. Yin, and Q. S. Yu: Applications of Electrospinning Technique in Drug Delivery. *Chem Eng Commun* **197** (10), 1315 (2010).
178. D. A. Brafman: Constructing stem cell microenvironments using bioengineering approaches. *Physiol Genomics* **45** (23), 1123 (2013).
179. Y. B. Zhang, J. P. Small, W. V. Pontius, and P. Kim: Fabrication and electric-field-dependent transport measurements of mesoscopic graphite devices. *Applied Physics Letters* **86** (7), (2005).